



U.S. DEPARTMENT OF
ENERGY



THE UNIVERSITY of
TENNESSEE **UT**

Investigation of Micro- and Macro-Scale Transport Processes for Improved Fuel Cell Performance

Department of Energy 2013 Annual Merit Review

Presented by Former PI:

Jon P. Owejan

SUNY Alfred

Current Project PI:

Wenbin Gu

General Motors

Electrochemical Energy Research Lab

May 15, 2013

This presentation does not contain any proprietary, confidential, or otherwise restricted information



Project ID # FC092

Overview

Timeline

- Project start date: June 2010
- Project end date: May 2013
(extended to Nov. 2013 at no cost)
- Percent complete: 85%

Budget

- Total project funding
 - DOE share: \$4.391M
 - Cost share: \$1.097M
- Funding received in FY11: \$1.15M
- Funding received in FY11: \$0.60M
- Funding received in FY12: \$1.48M
- Planned Funding for FY13: \$1.16M

Barriers

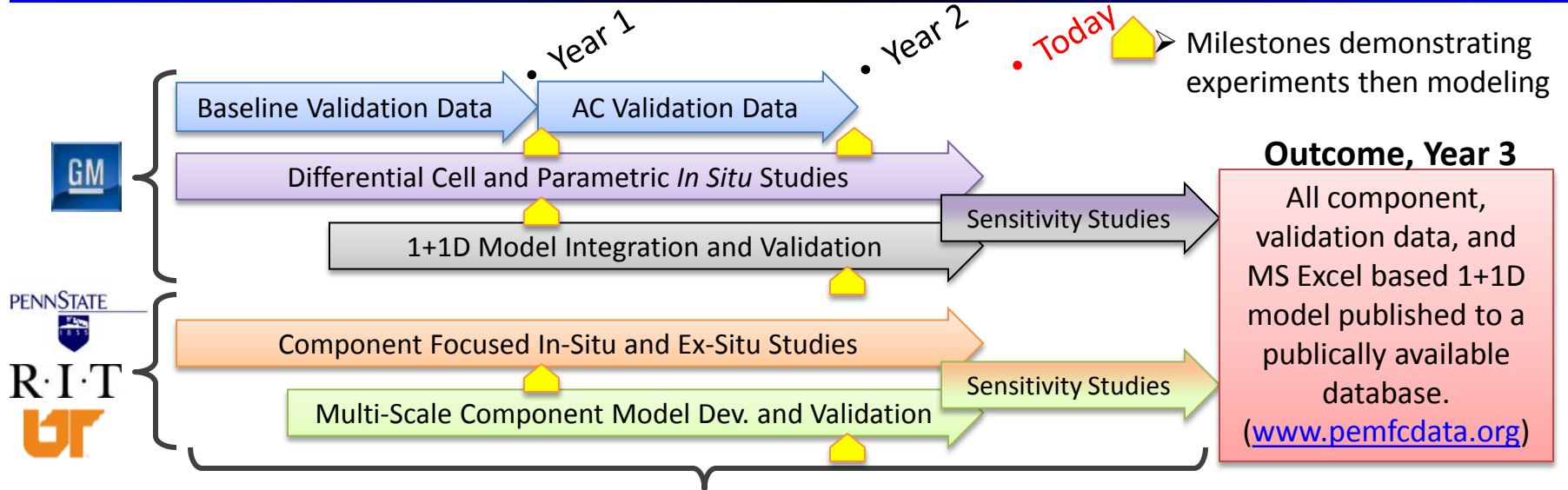
- Barriers addressed
 - C. Performance
 - D. Water Transport within the Stack
 - E. System Thermal and Water Management
 - G. Start-up and Shut-down Time and Energy/Transient Operation

Partners

- Project lead: General Motors
- Subcontract Partners:
 - Rochester Inst. of Technology
 - Univ. of Tenn. Knoxville
 - Penn State University
- Other collaborations with material suppliers

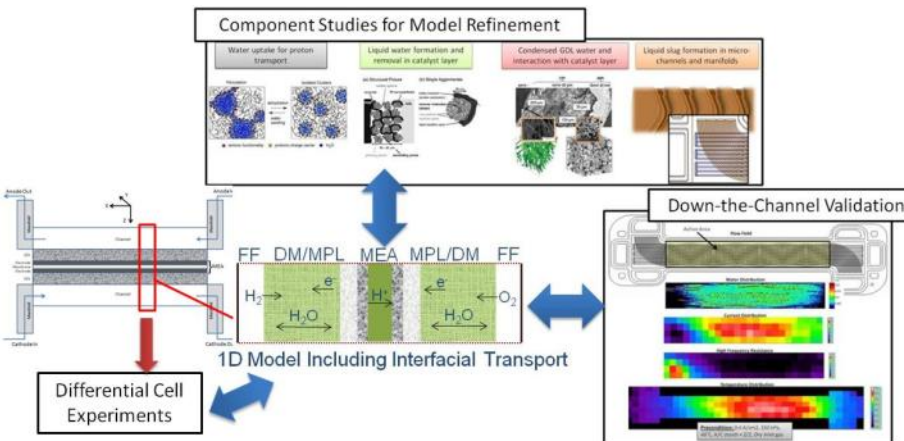
Approach-

Connecting Characterization Techniques with a Validated 1+1D Model



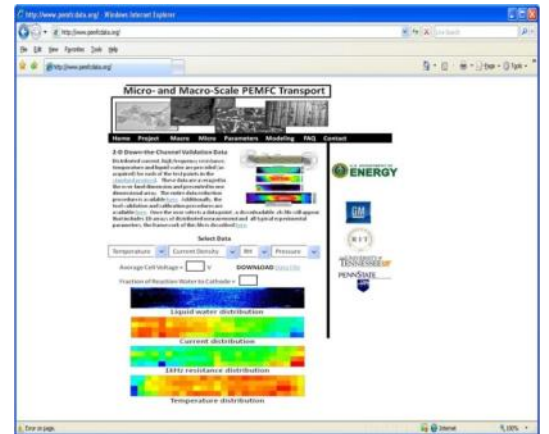
All work streams connected by the transport resistance associated with a component of:

$$E_{\text{cell}} = E_{\text{rev}} - \eta_{\text{HOR}} - |\eta_{\text{ORR}}| - i \cdot R_{\text{tx},e^-} - i \cdot R_{\text{tx},\text{Mem.}} - i \cdot R_{\text{tx},\text{H}^+} - \eta_{\text{tx},\text{O}_2(\text{Ch})} - \eta_{\text{tx},\text{O}_2(\text{GDL})} - \eta_{\text{tx},\text{O}_2(\text{electrode})}$$



Dry Model Starting Point:
 W. Gu *et al.*, "Proton exchange membrane fuel cell (PEMFC) down-the-channel performance model," *Handbook of Fuel Cells* - Volume 5, Prof. Dr. W. Vielstich *et al.* (Eds.), John Wiley & Sons Ltd., (2008).

Database: www.PEMFCdata.org



Collaboration

- **GM Electrochemical Energy Research Lab (prime):** Wenbin Gu, Jeffrey Gagliardo, Anu Kongkanand, Vinod Kumar
- **Formerly GM:** Paul Nicotera, Jeanette Owejan, Rob Reid
- **Penn State University (sub):** Michael Hickner
- **Rochester Institute of Tech (sub):** Satish Kandlikar, Thomas Trabold
- **University of Tennessee (sub):** Matthew Mench
- **University of Rochester (sub):** Jacob Jorne'
- **DOE Transport Working Group**
- **National Institute of Standards and Technology (no cost):** David Jacobson, Daniel Hussey, Muhammad Arif
- **W.L. Gore and Associates, Inc. (material cost):** Simon Cleghorn
- **Freudenberg (material cost):** Christian Quick
- **Engineered Fiber Technologies (material cost):** Robert Evans
- **Queens University (no cost):** Kunal Karan
- **Carnegie Mellon University (no cost):** Shawn Litster
- **SUNY Alfred State (no cost):** Jon Owejan

Core Objectives Addressing DOE Expectations

Topic 4a - Expected Outcomes:

- Validated transport model including all component physical and chemical properties
 - Down-the-channel pseudo-2D model will be refined and validated with data generated in the project
- Public dissemination of the model and instructions for exercise of the model
 - Project website to include all data, statistics, observation, model code and detailed instructions
- Compilation of the data generated in the course of model development and validation
 - Reduced data used to guide model physics to be published and described on project website
- Identification of rate-limiting steps and recommendations for improvements to the plate-to-plate fuel cell package
 - Model validation with baseline and auto-competitive material sets will provide key performance limiting parameters

Characterization and validation data

Employing new and existing characterization techniques to measure transport phenomena and fundamentally understand physics at the micro-scale is the foundation of this project. Additionally, a comprehensive down-the-channel validation data set is being populated to evaluate the integrated transport resistances. This work will consider a baseline and next generation material set.

Multi-Scale component-level models

Models that consider bulk and interfacial transport processes are being developed for each transport domain in the fuel cell material sandwich. These models will be validated with a variety of *in situ* and *ex situ* characterization techniques. One dimensional transport resistance expressions will be derived from these models. This work will consider a baseline and next generation material set.

1+1D fuel cell model solved along a straight gas flow path

Consider if a 1+1D simplified model can predict the saturation state along the channel, performance and the overall water balance for both wet and dry operating conditions within the experimental uncertainty of the comprehensive macro-scale validation data sets. Identify shortcomings of 1D approximations.

Identify critical parameters for low-cost material development

Execute combinatorial studies using the validated model to identify optimal material properties and trade-offs for low-cost component development in various operating spaces.

Project Standardization

Baseline Material Set

- Membrane
 - Gore® 18 μm
- Anode catalyst layer
 - target loading 0.05 $\text{mg}_{\text{Pt}} \text{cm}^{-2}$
 - 20% Pt/V made with 950EW ionomer I/C 0.6
- Cathode catalyst layer
 - target loading 0.3 $\text{mg}_{\text{Pt}} \text{cm}^{-2}$
 - 50% Pt/V made with 950EW ionomer I/C 0.95
- Microporous layer
 - 8:1:1 carbon-to-PTFE-to-FEP ratio, 30 μm thick
- Gas diffusion substrate
 - MRC 105 w/ 5% wt. PTFE, 230 μm thick w/MPL
- Flow field
 - 0.7 mm wide by 0.4 mm deep channels with stamped metal plate cross-sectional geometry
 - 18.3 cm channel length
 - 0.5 mm cathode land width
 - 1.5 mm anode land width
 - Exit headers typical to a fuel cell stack

Auto-Competitive Material Set

- Membrane
 - Gore® 12 μm
- Anode catalyst layer
 - target loading 0.05 $\text{mg}_{\text{Pt}} \text{cm}^{-2}$
 - 20% Pt/V with 950EW ionomer I/C 0.6
- Cathode catalyst layer
 - target loading 0.1 $\text{mg}_{\text{Pt}} \text{cm}^{-2}$
 - 15% Pt/V with 950EW ionomer I/C 0.7
- Microporous layer
 - 8:1:1 carbon-to-PTFE-to-FEP ratio, 30 μm thick
- Gas diffusion substrate
 - Anode – prototype high diffusion res, w/ 5% wt. PTFE, 210 μm thick w/MPL
 - Cathode - MRC 105 w/ 5% wt. PTFE, 230 μm thick w/MPL
- Flow field
 - 0.7 mm wide by 0.3 mm deep channels with stamped metal plate cross-sectional geometry
 - 18.3 cm channel length
 - 0.25 mm cathode land width
 - 0.75 mm anode land width
 - Modified exit headers

Standard Protocol 4 x 4 x 3 x 3 Factors

Temperature

20, 40, 60, 80°C

Inlet RH (An/Ca)

95/95, 0/95, 95/0, 50/50%

Outlet Pressure (An/Ca)

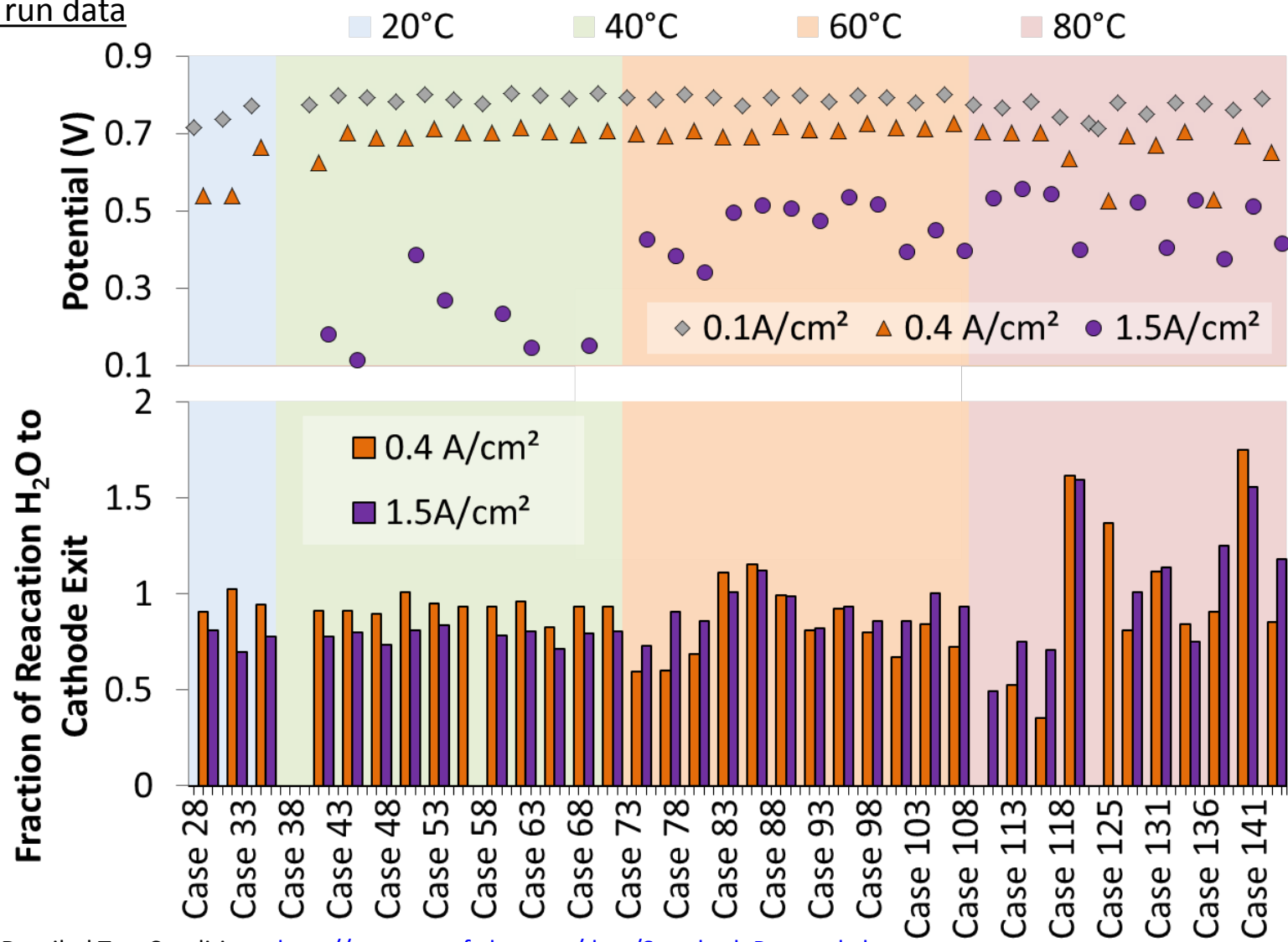
150/150, 100/150, 150/100 kPa

Current Density

0.1, 0.4, 1.5 A/cm^2

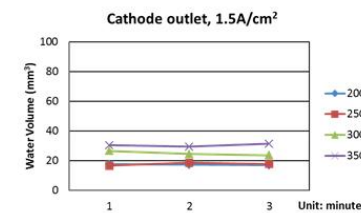
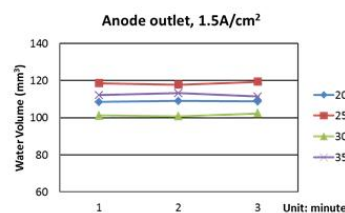
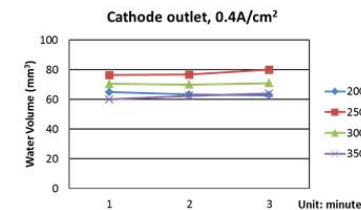
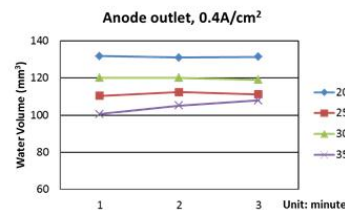
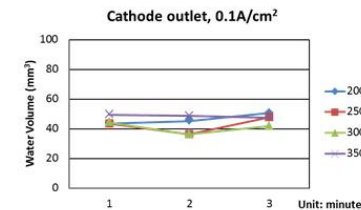
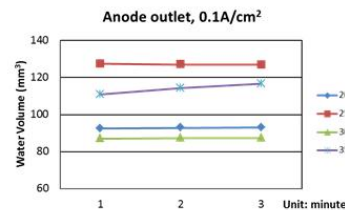
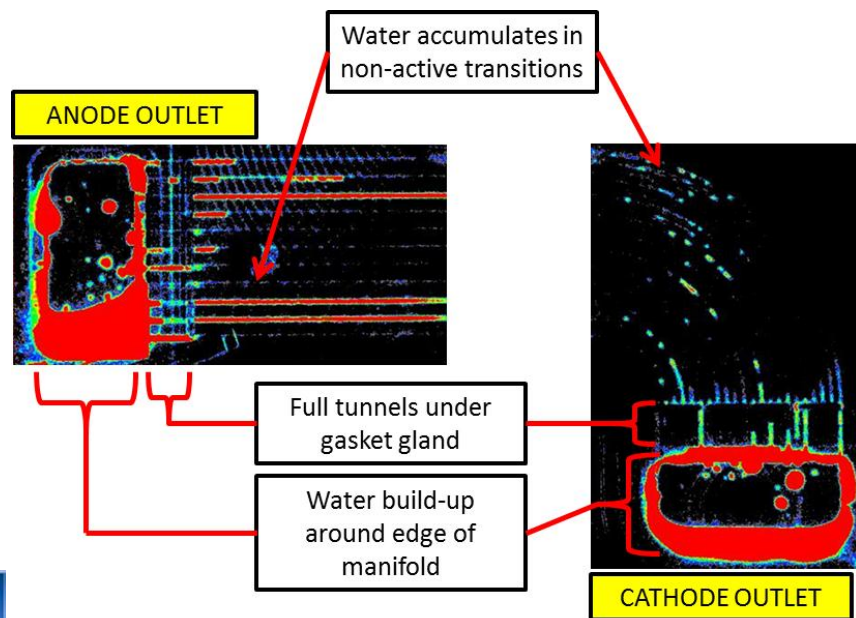
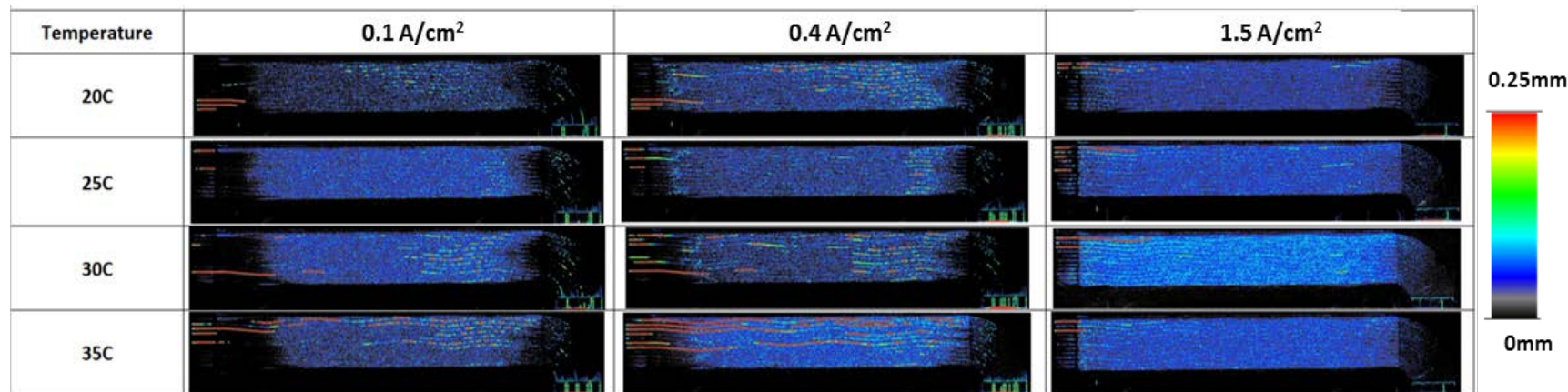
Completion of Auto-Competitive Validation Dataset

First run data



Detailed Test Conditions: http://www.pemfcdata.org/data/Standard_Protocol.xls

- Studied active and non-active area water volumes as a function of cell temperature and current density.



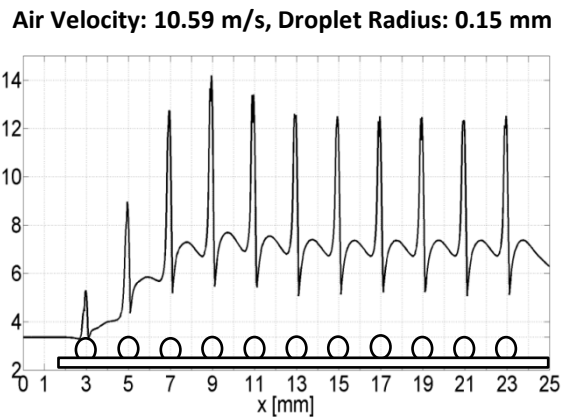
The Effect of Droplets and Films on Interfacial O₂ Resistance

Fully developed Sh=3.35 (Baseline Channels)

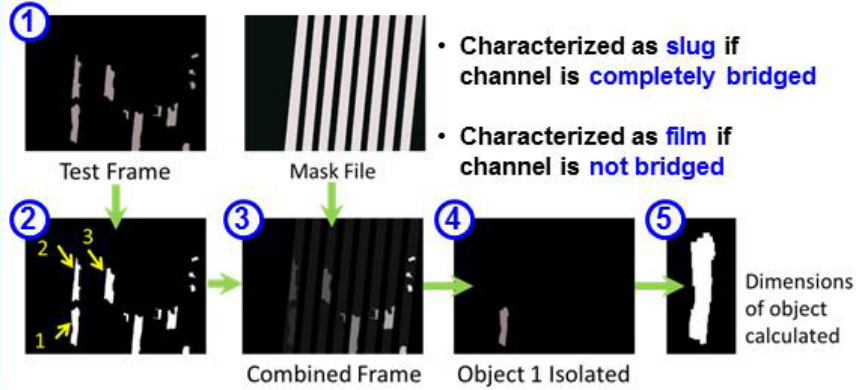
Multiple Droplets



- Significant increase in Sh for the first 4 droplets
- Average Sh increases to 123%

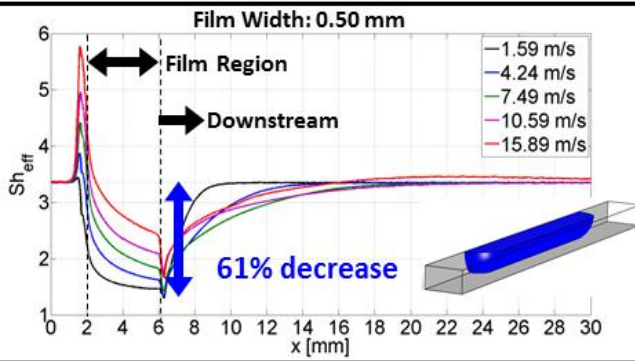


Flow Pattern Identification

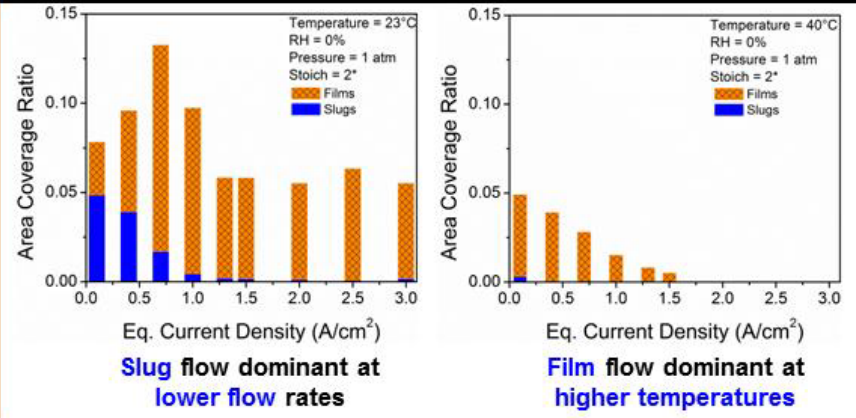


Films - Air Velocity

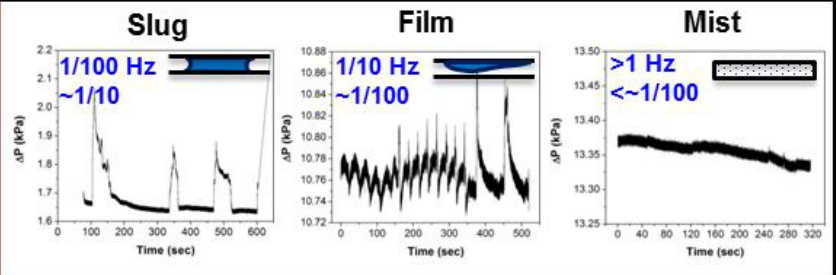
Air velocity impacts Sh_{eff} positively in the film region and negatively in the wake region. Decrease in Sh_{eff} persists in film wake for ~1-2 film lengths



Flow Pattern Trends



Flow Patterns



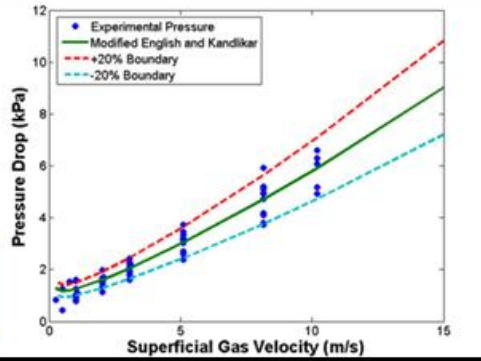
2φ ΔP Correlation

$$\Delta P_{TP} = \Delta P_G \phi_G^2$$

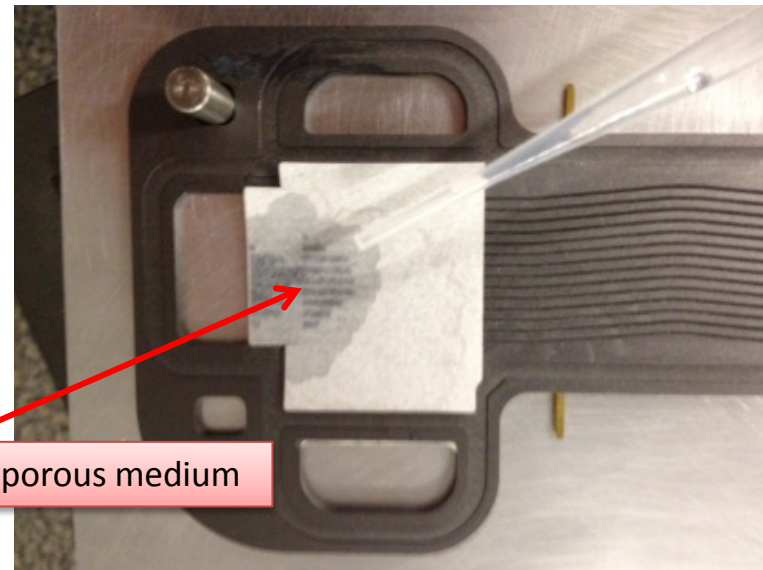
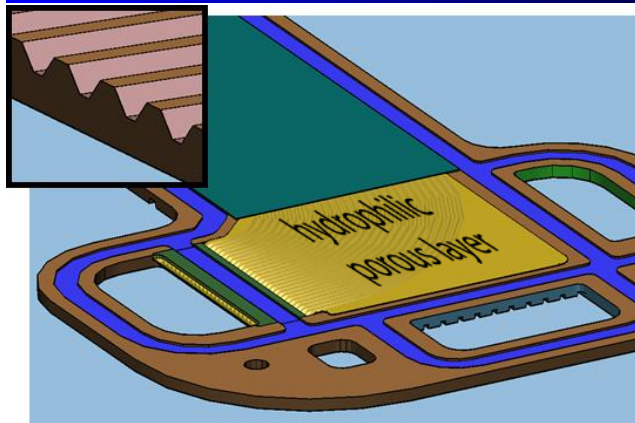
$$\phi_G^2 = 1 + CX + X^2$$

$$X = \left(\frac{\rho_G}{\rho_L}\right)^{0.5} \left(\frac{\mu_L}{\mu_G}\right)^{0.1} \left(\frac{1-x}{x}\right)^{0.9}$$

$$C = A \left(\frac{1-x}{x}\right)^b \quad \begin{matrix} A = 0.0856(u_L)^{-1.202} \\ b = 0.004(u_L)^{-0.526} \end{matrix}$$

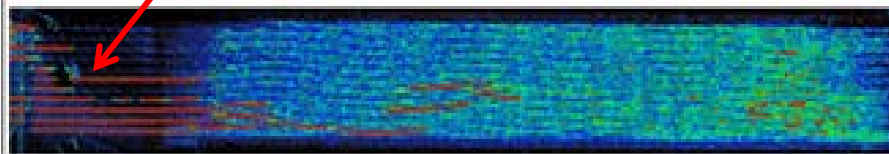


Auto-Competitive Design Outlet Water Management

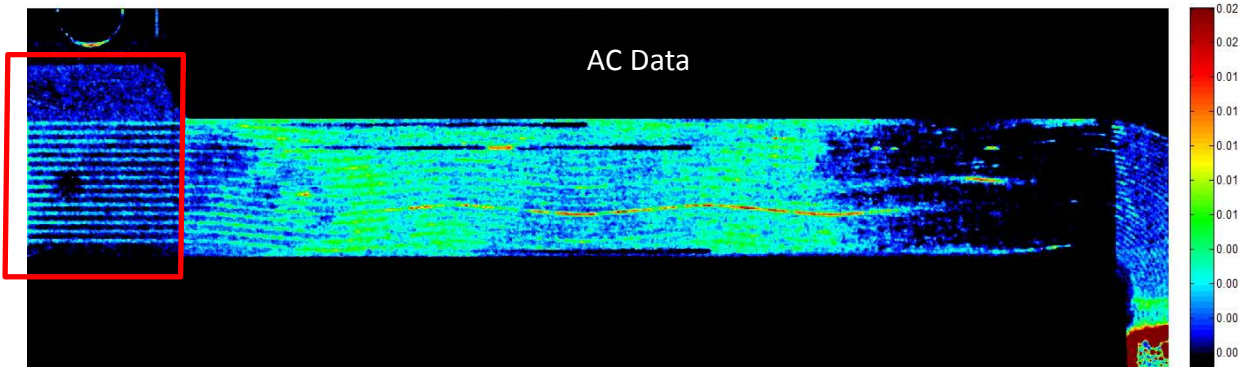


Water slugs are reduced by wicking liquid water into hydrophilic porous medium

Baseline Data

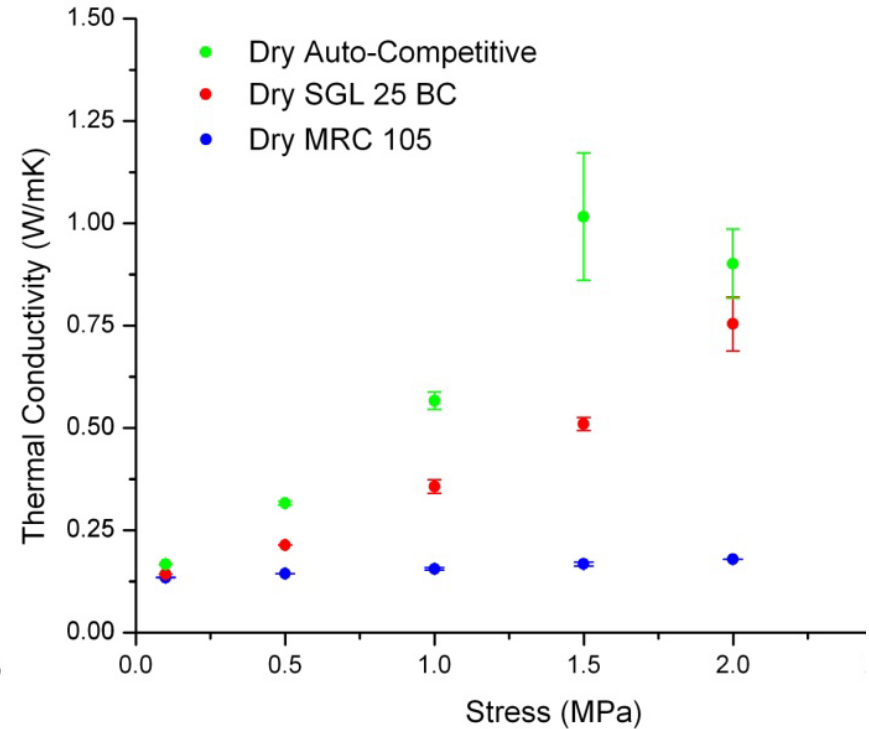
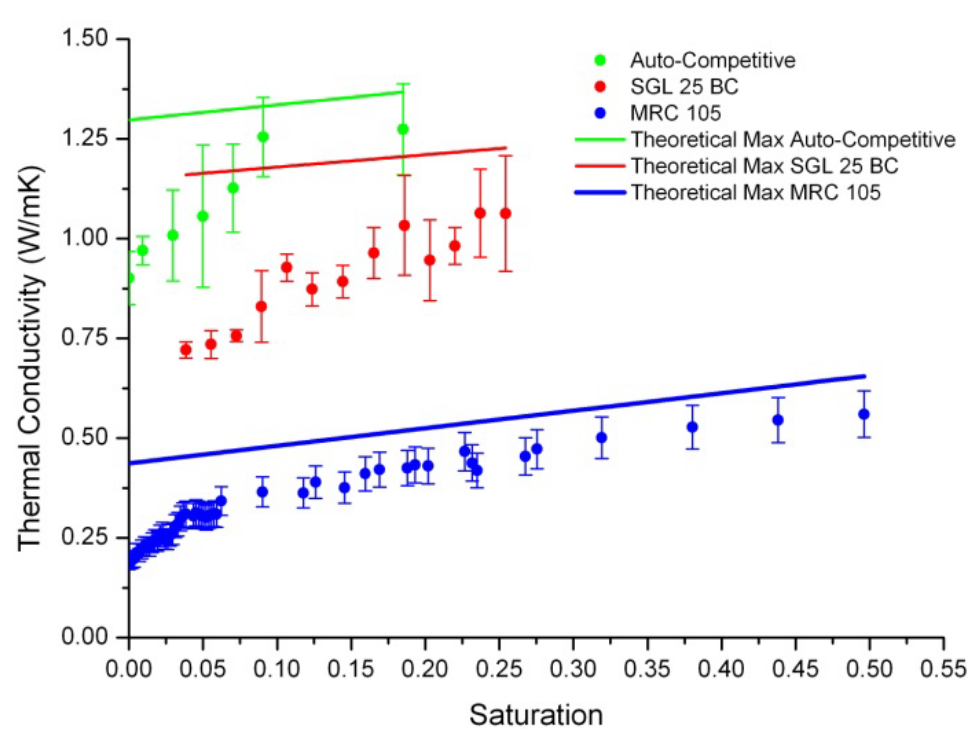


AC Data



Neutron imaging experiments demonstrate AC outlet design decreasing water accumulation at the outlet. From a dry state this design prevents slug blockage for 1 to 5 minutes (dependent on operating conditions).

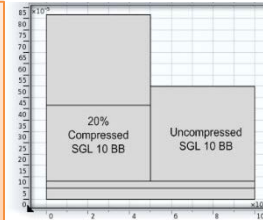
GDL Thermal Conductivity Dependence on Saturation



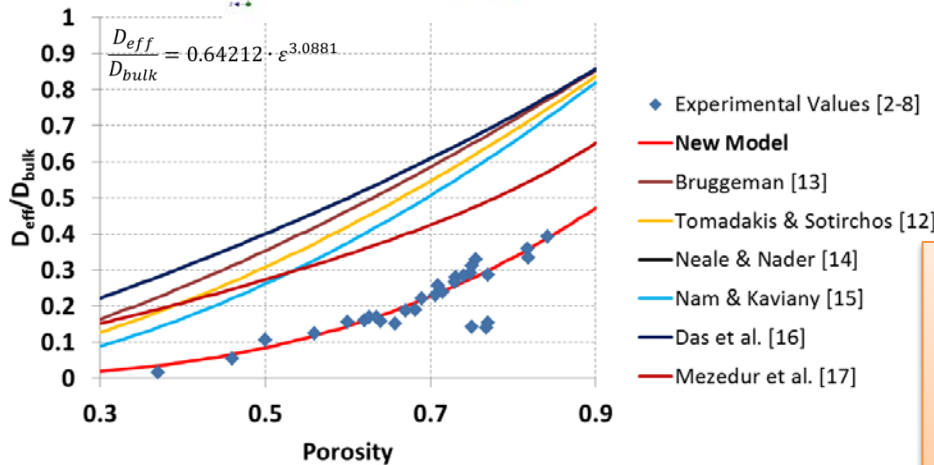
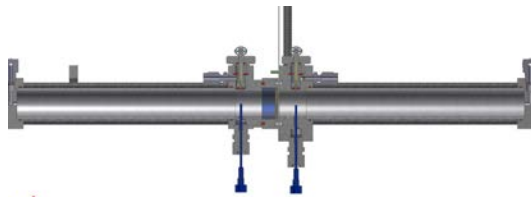
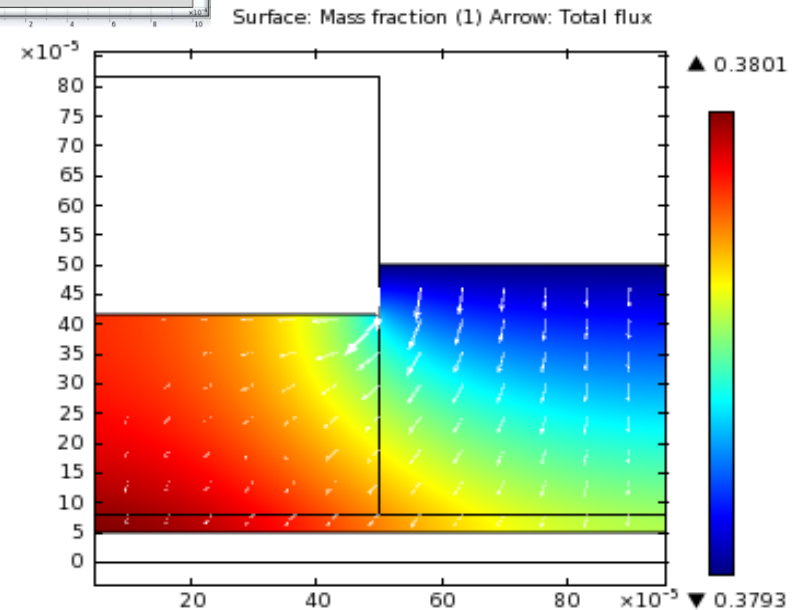
- Thermal conductivity relationships deduced; increase as saturation levels increase.
- Theoretical maximum of conductivity based on completely connected pores, and departure represents non-aligned/connected liquid.
- Compression has significant impact on Auto-Competitive material sets but not on baseline materials.
- Stress-strain relationships for all materials used for correction of measured k_{th} .
- The presence of micro-porous layer doesn't change composite thermal conductivity much.

Saturated GDL Mass Diffusivity and GDL Component Model

- A Loschmidt diffusion cell has been designed and built to measure the effective diffusion coefficients of partially saturated porous samples.
- A new analytical solution method has been developed that simplifies diffusion cell design, enables a much more compact design with high precision. A new D_{eff}/D_{bulk} semi-empirical model for dry media was developed by using a compilation of data in literature.



Data from Neutron Imaging and Limiting Current Study Used in Model



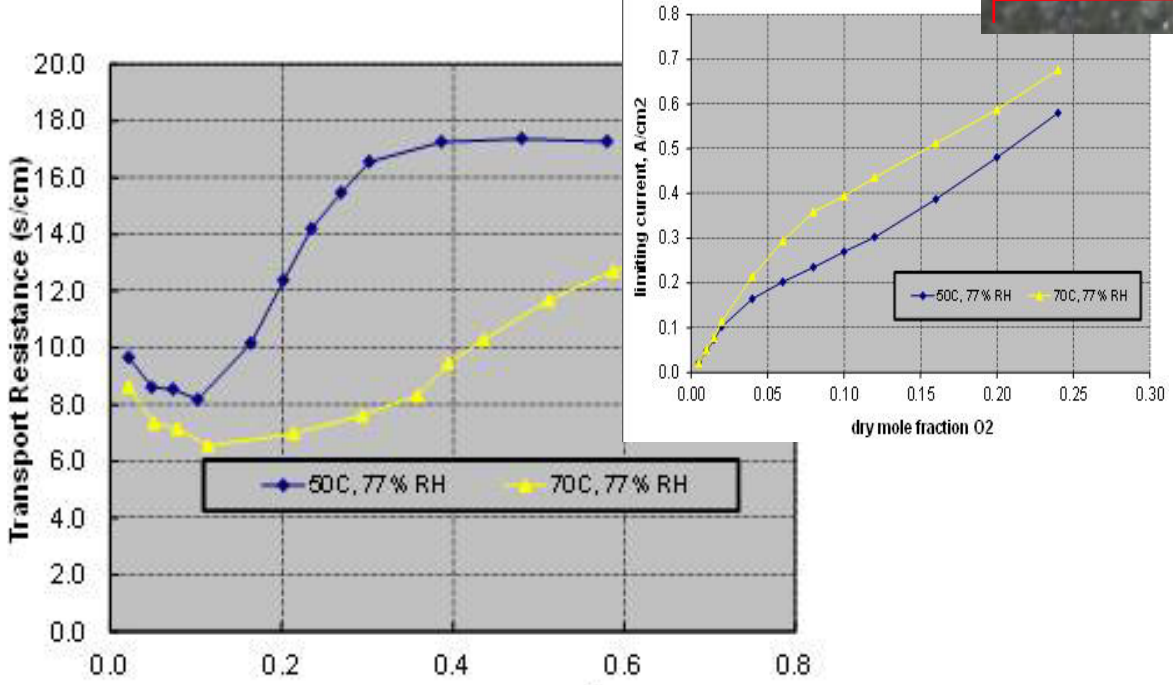
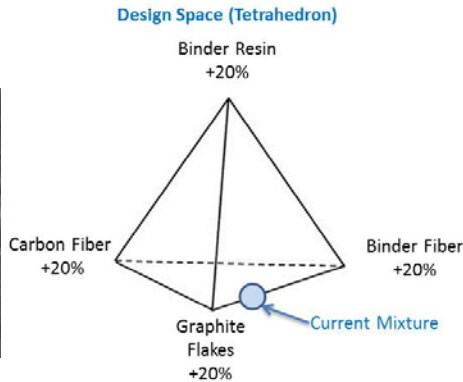
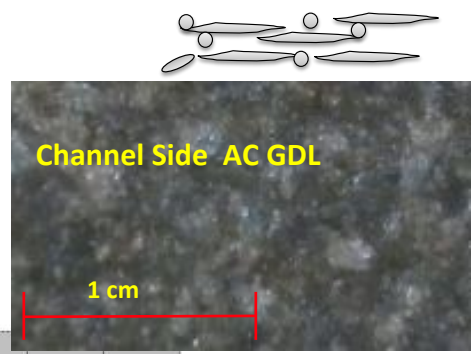
Semi-Empirical Model Developed for Dry Media

- A component level model for the numerical simulations of the GDL Component is in development.
- Inclusion of phase change flow, capillary flow, and multi-component diffusion of gas into homogeneous porous saturated media representing GDL.
- Future step is integration of μ x-ray 3D tomograph into computational domain.

Auto-Competitive GDL Transport Properties

- Concurrently with the quaternary mixture study for mechanical properties, each of the study samples was also tested for its transport properties.
- Data analysis is in progress.
- Preliminary AC GDL diffusivity values as follows:

$$\left(\frac{D}{D_{eff}}\right)_{wet} : 50 \quad \left(\frac{D}{D_{eff}}\right)_{dry} : 20$$

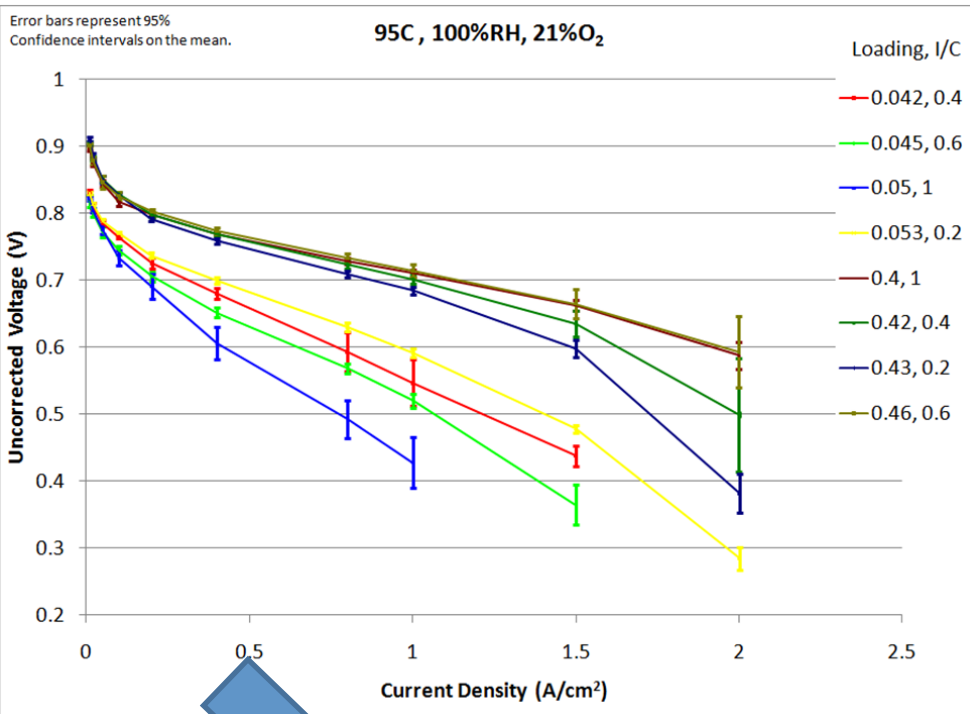


Property Targets

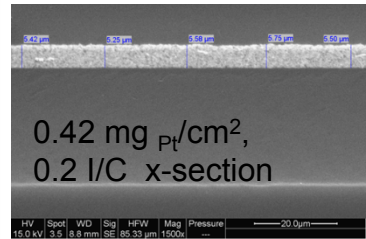
- Tortuosity > 7
- Compressibility < 30% strain at 2 MPa of compressive stress
- Shear modulus > 10 MPa

| Mixture | Fraction of 20 wt.% Being Varied | | | |
|---------|----------------------------------|-----------------|--------------------------|--------------|
| | Carbon Fiber | Graphite Flakes | Fibrillated Fiber Binder | Resin Binder |
| Current | 0.00 | 0.75 | 0.25 | 0.00 |
| 1 | 1.00 | 0.00 | 0.00 | 0.00 |
| 2 | 0.00 | 1.00 | 0.00 | 0.00 |
| 3 | 0.00 | 0.00 | 1.00 | 0.00 |
| 4 | 0.00 | 0.00 | 0.00 | 1.00 |
| 5 | 0.50 | 0.50 | 0.00 | 0.00 |
| 6 | 0.50 | 0.00 | 0.50 | 0.00 |
| 7 | 0.50 | 0.00 | 0.00 | 0.50 |
| 8 | 0.00 | 0.50 | 0.50 | 0.00 |
| 9 | 0.00 | 0.50 | 0.00 | 0.50 |
| 10 | 0.00 | 0.00 | 0.50 | 0.50 |
| 11 | 0.33 | 0.33 | 0.33 | 0.00 |
| 12 | 0.33 | 0.33 | 0.00 | 0.33 |
| 13 | 0.33 | 0.00 | 0.33 | 0.33 |
| 14 | 0.00 | 0.33 | 0.33 | 0.33 |
| 15 | 0.25 | 0.25 | 0.25 | 0.25 |

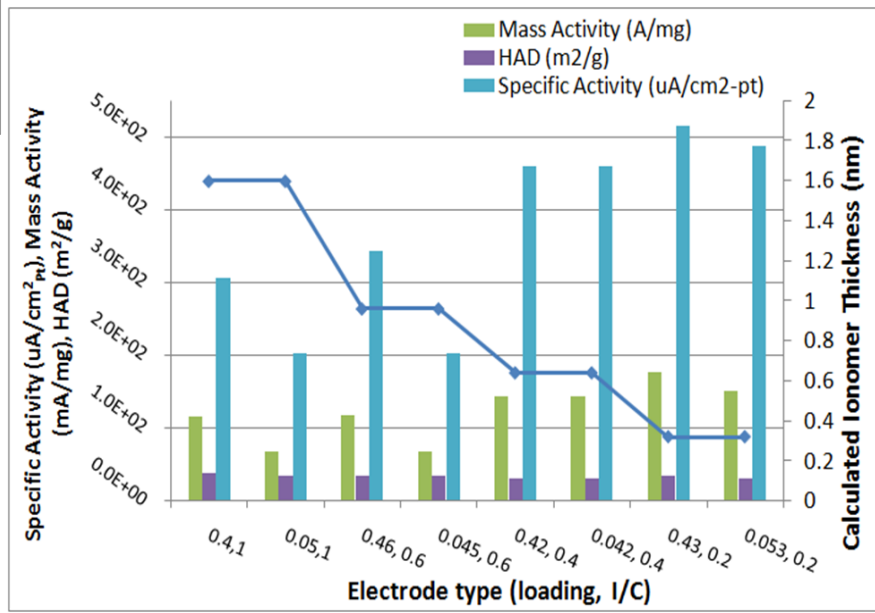
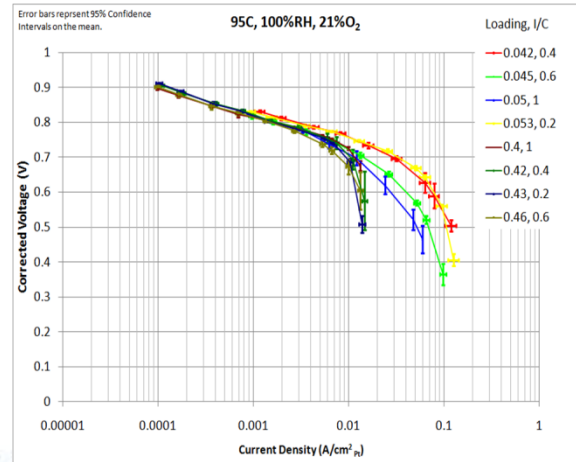
Impact of Ionomer Film Thickness on Voltage Loss



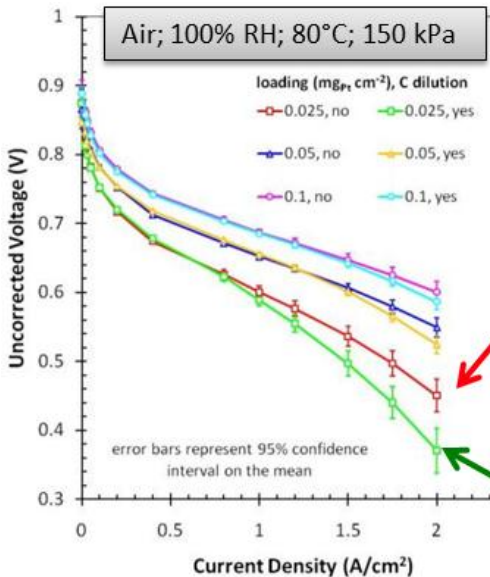
By decreasing the ionomer film thickness on the catalyst particle, it is possible to decrease the oxygen transport resistance. This is verified by studying two catalyst loadings. Ultimately, a tradeoff between this and proton transport resistance would determine optimized I/C for a given set of operating conditions.



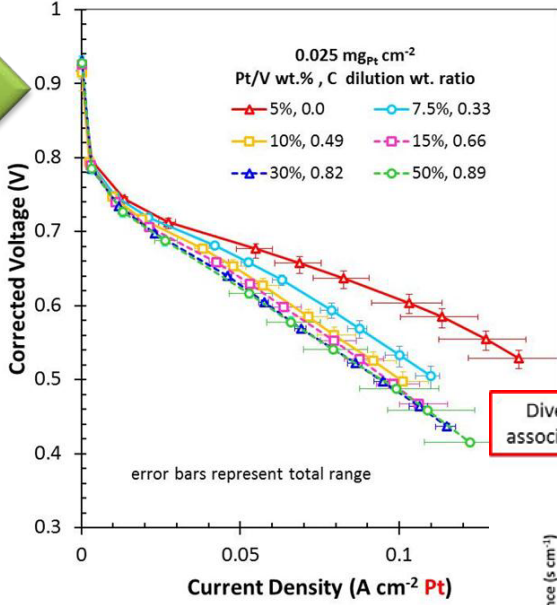
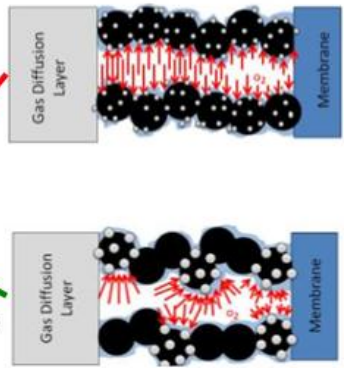
Performance improvement not associated with Pt surface variations – verifies impact of film thickness (with all voltage loss accounted for).



Technical Accomplishments- Considering Interfacial Resistance with Analysis at a Single Pt Particle

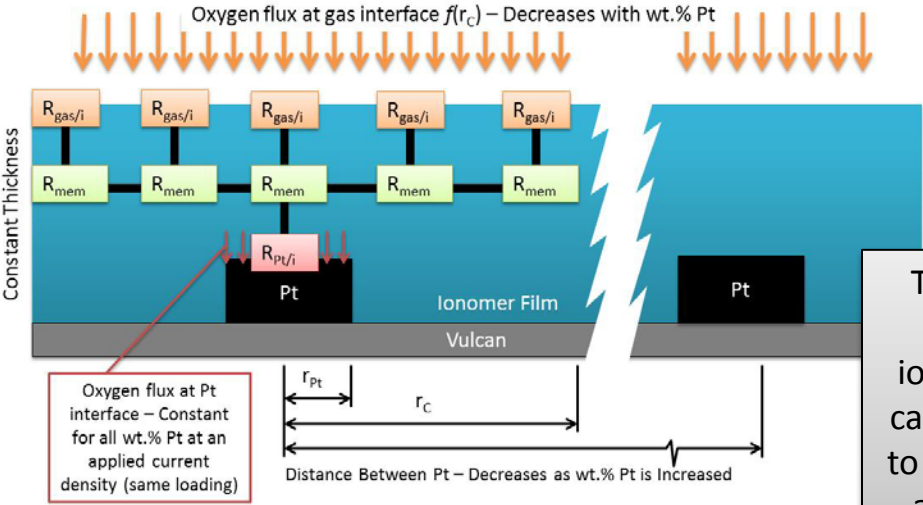


Ohmic, sheet resistance, x-over, bulk transport corrected and normalized to Pt area



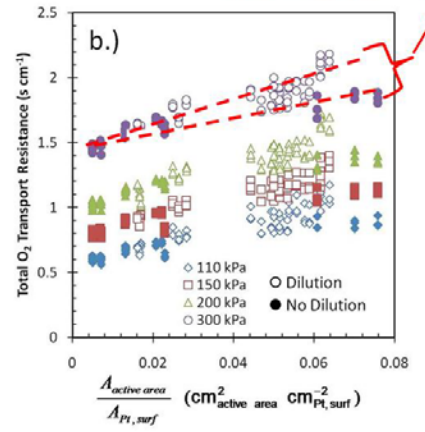
ECSA measurement is critical for this normalization. Validated with XRD and TEM analyses.

Divergence indicates resistance is not associated exclusively with the Pt surface.



$$R_{O_2, local}^e = \frac{\delta_{equiv}}{K_{O_2} RT}$$

$\delta_{equiv} \sim 20-40 \text{ nm}$
(not possible, should be $\sim 4 \text{ nm}$)



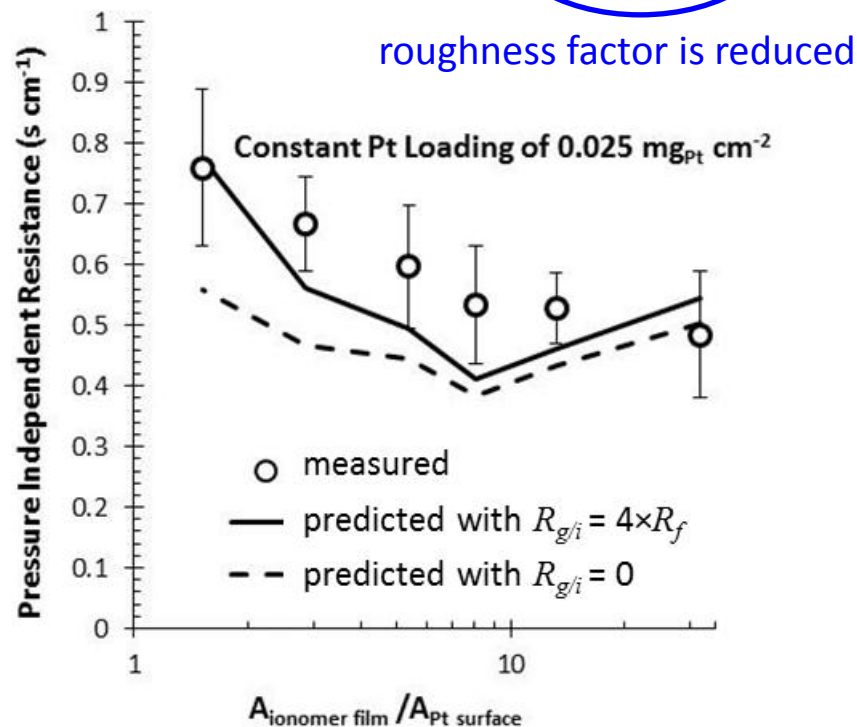
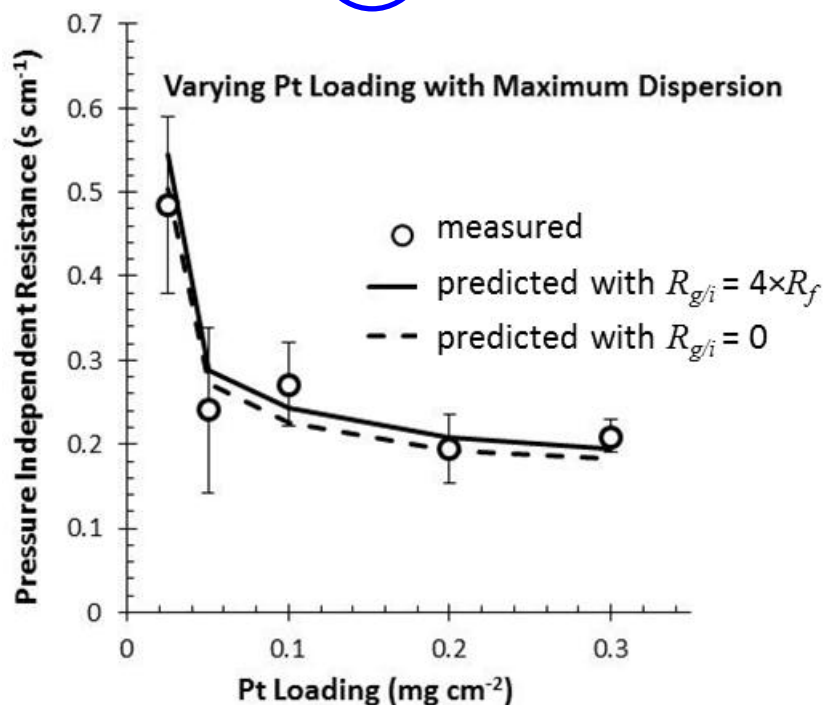
To consider the relative impact of bulk (R_{mem}), gas interfacial ($R_{gas/i}$), and Pt interfacial ($R_{Pt/i}$) resistances in the thin film ionomer. For a given P_{O_2} , the limiting current at the particle is calculated and the associated transport resistance is compared to measured results by assuming a uniform current distribution across all particles. Varying R_{mem} vs R_{gas} vs R_{Pt} highlights the physical nature of the observed transport resistance.

Correlating Local Resistance to Pt and Ionomer Film Surface Area

Inverse of roughness factor

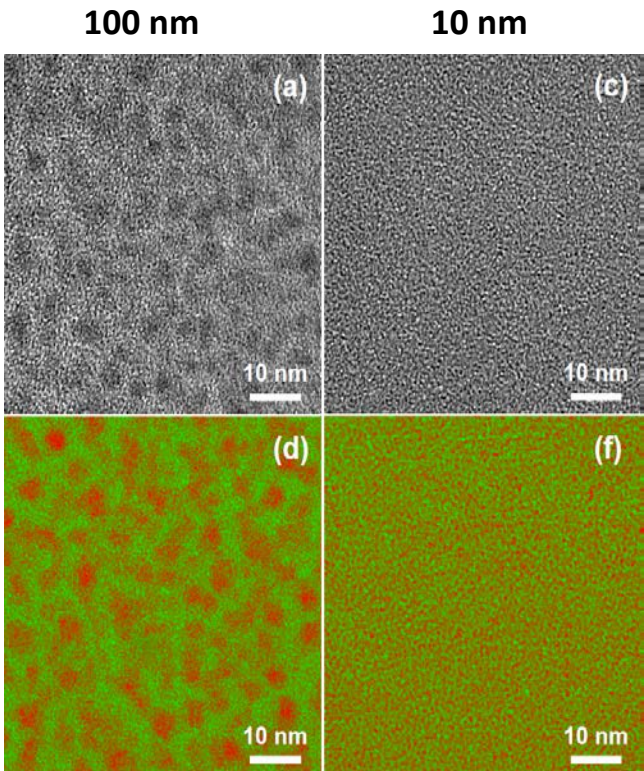
$$R_{O_2}^{P,ind} = R_{O_2}^{Knudsen} + \frac{A_{electrode}}{A_{Pt,surface}} R_{O_2}^{local}$$

$$R_{O_2}^{P,ind} = R_{O_2}^{Knudsen} + \frac{A_{electrode}}{A_{Pt,surface}} R_{O_2}^{Pt/i} + \frac{A_{electrode}}{A_{Ionomerfilm}} R_{O_2}^{g/i} \approx R_{O_2}^{Knudsen} + \left(\frac{A_{electrode}}{A_{Pt,surface}} + \frac{A_{electrode}}{A_{Ionomerfilm}} \right) R_{O_2}^{local}$$

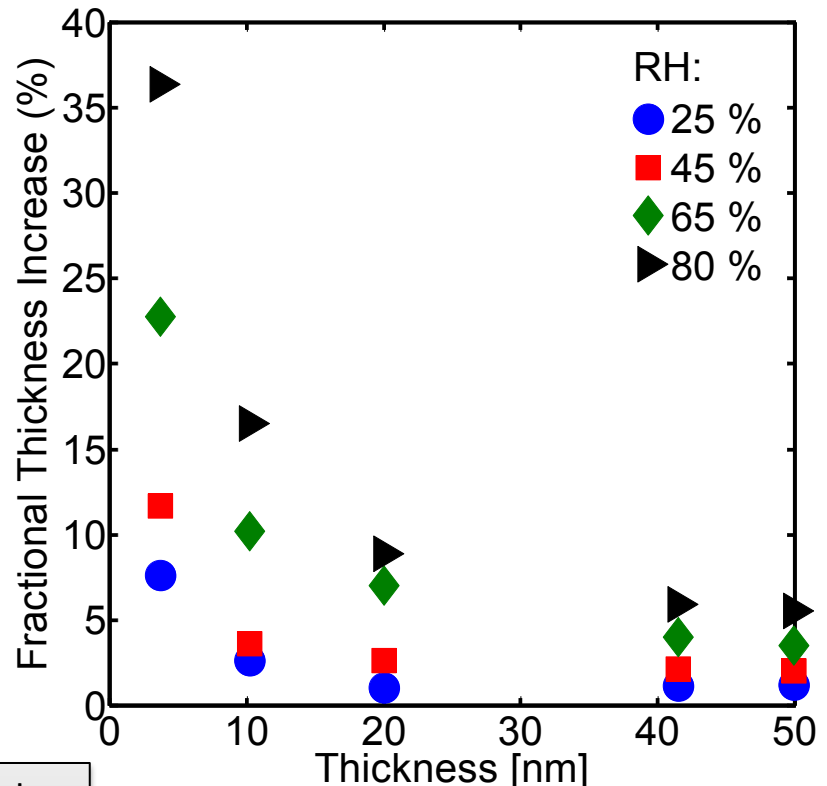


- $R_{Pt/i} = 4 \times R_f$ is used to match the measured local oxygen transport resistance.
- For better agreement to the trend in the resistance as the area of ionomer film surface increases, one needs to use interfacial resistances at both Pt/ionomer and gas ionomer interfaces.

Swelling and Domain Structure in Thin Films



TEM from A. Weber



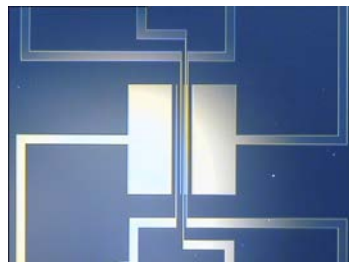
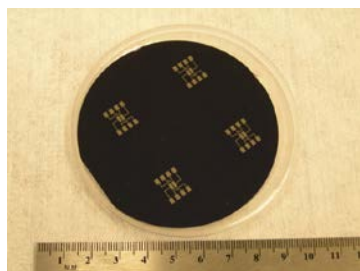
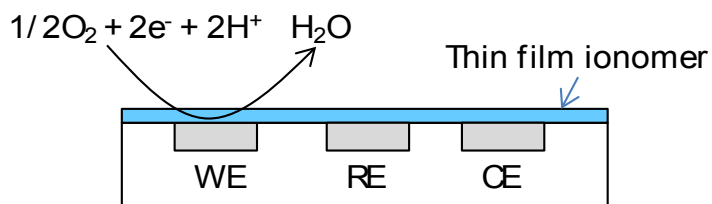
Ionic domain structure is altered in thin films which will lead to different transport properties. Small domains in thin films decrease the proton conductivity and may change the nature of the catalyst particle/ionomer interface. Thin films show much higher swelling on Si surfaces which may be due to less hydrophobic reinforcement because of limited/no ionic domain structure.

Modestino, M. A., F. I. Allen, D. K. Paul, S. K. Dishari, S. A. Petrina, M. A. Hickner, K. Karan, A. M. Minor, R. A. Segalman, A. Z. Weber, "Self-assembly and transport limitations in confined Nafion films," *Macromolecules* **2013**, 46(3), 867–873.

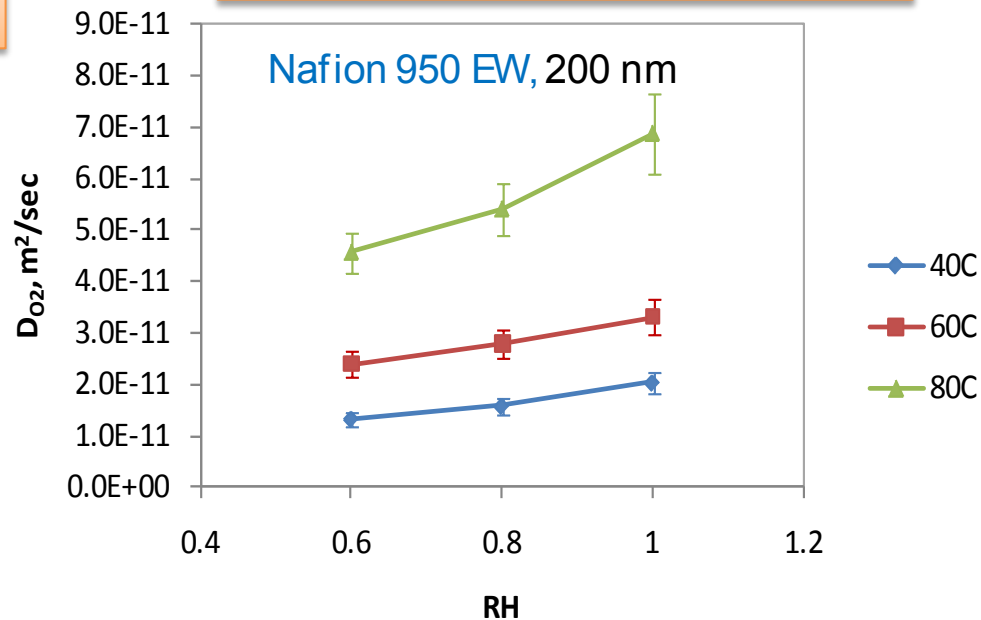
Measuring O₂ Transport in Ionomer Thin Film

- Use flat model electrode to measure intrinsic transport properties of ionomer without convolution of a porous medium.
- Experiment done on microelectrode coated with 100nm thick ionomer showed comparable bulk O₂ transport resistance to that of thick (>10μm membrane) membranes.
- However, the measurement on thinner ionomer thickness was unreliable due to coating and characterization techniques (want ~10nm, similar to electrode).
- The thin films appear to be porous in the experiments, making it incredibly difficult to measure O₂ diffusion on a large/flat electrode.
 - need to use nanoparticles to simulate the particle/film interface.

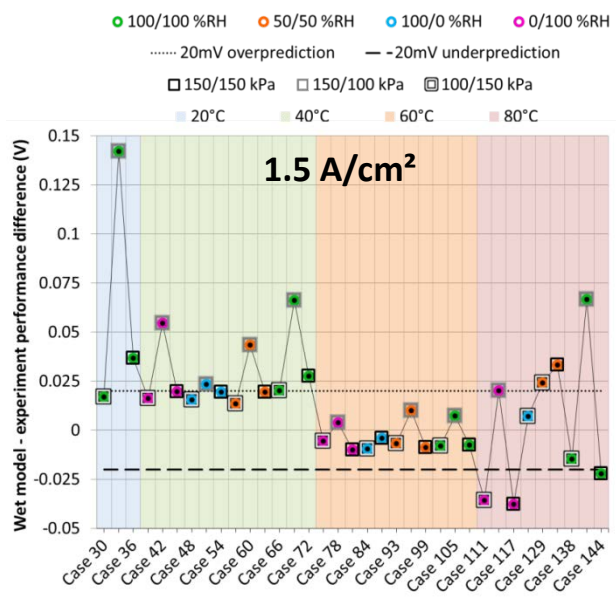
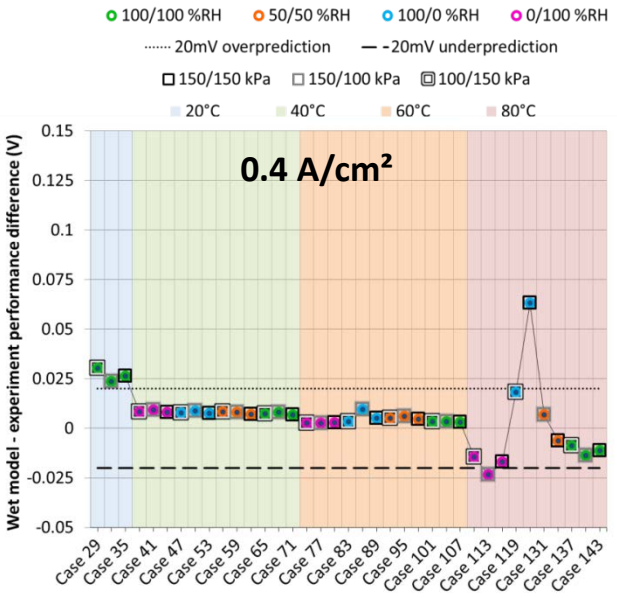
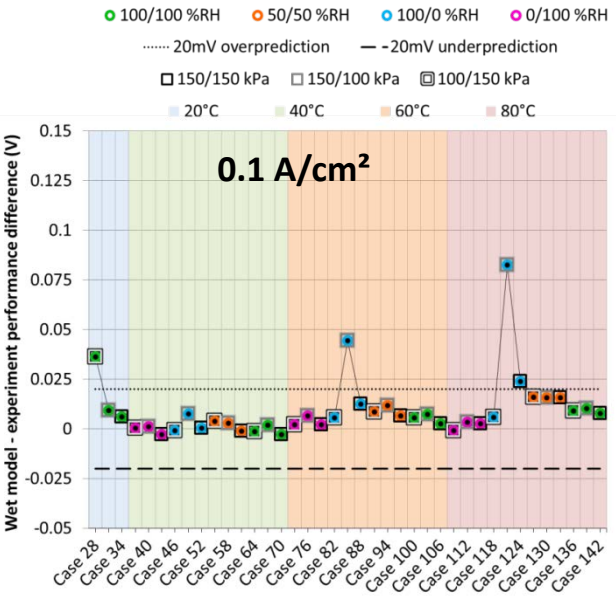
Measure transport properties in thin ionomer film using O₂ diffusion-controlled limiting current



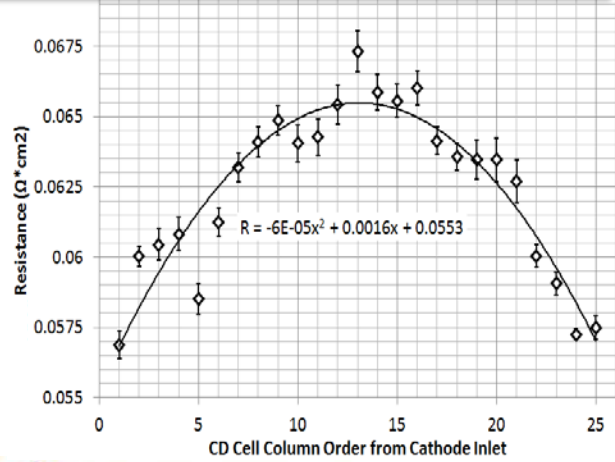
O₂ diffusion coefficient in 200nm Nafion®



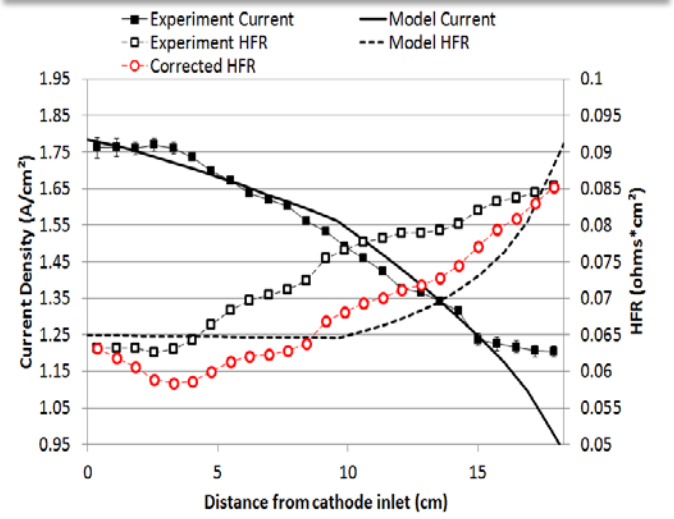
Current Status of Wet 1+1D Model – Baseline Material Set – Error



Down-the-Channel Resistance Variation



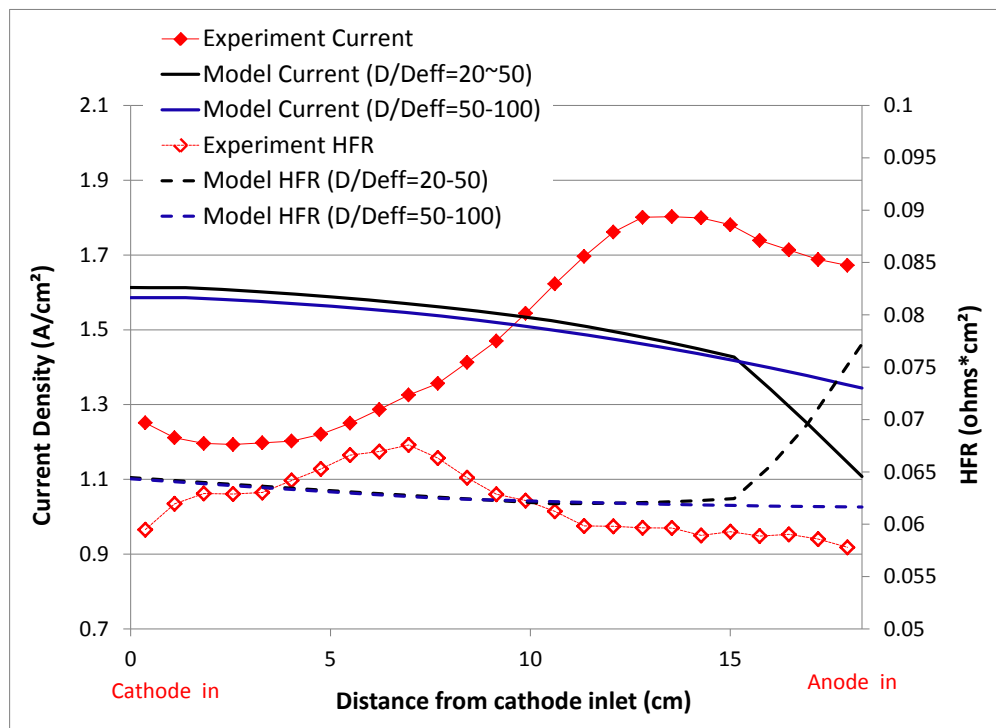
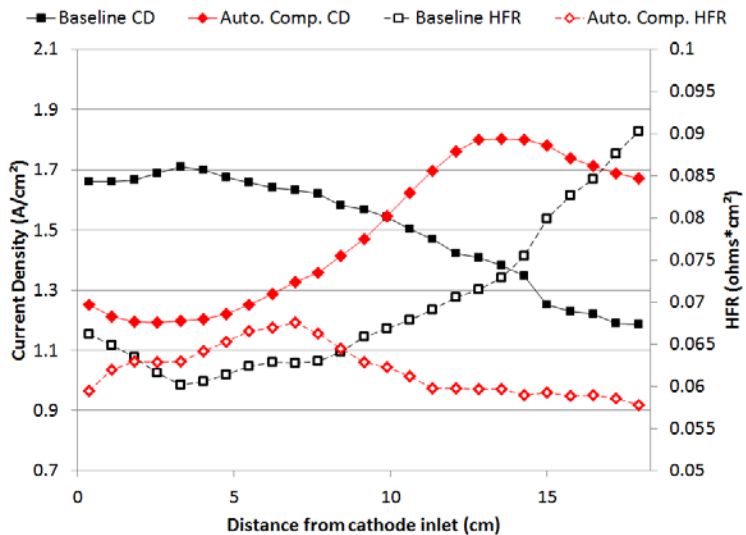
Data/Model Comparison with Correction



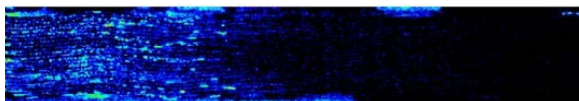
The accuracy of predicted HFR was improved by characterizing compression effects that result from the printed circuit board used for distributed measurements. Overall, the 1+1D model predicts performance within experimental uncertainty for the majority of operating conditions investigated.

Model-Data Comparisons – AC Material Set

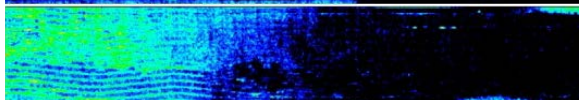
60°C ,H2/Air, 1.5/2 stoich, 0/95 %RH, 1.5 A/cm²



Baseline
WB = 0.52



Auto Comp.
WB = 0.71



| Anode D/Deff (dry - wet) | 2.8 - 5.6 | 20 - 50 | 50 - 100 |
|--------------------------------------|-----------|---------|----------|
| Fraction of product water to cathode | 0.48 | 0.69 | 0.79 |

- Higher diffusion resistance Anode GDL forces more product water to move cathode flow-field and membrane is more uniformly humidified. The model predicts the same trend.
- AC material set yields a more flooded cathode catalyst layer and results in an opposite trend in current distribution. The model needs to address liquid water saturation issue in the electrode (with low Pt loading in particular).

Summary

- **Baseline validation data set is complete with 95% confidence intervals and auto-competitive validation data set is near completion**
 - 95% confidence intervals for the mean established for performance metrics by 3 separate experimental runs of the project standard protocol.
 - AC experiments show a significant impact of high diffusion resistance anode GDL on water balance and current & HFR distributions.
- **Several 1-D relationships have been established and refined for use in the 1+1D model**
 - Channel-to-manifold two-phase pressure drop as a function of water volume.
 - GDL/channel interfacial O_2 transport resistance relating to Area Coverage Ratio (ACR) and two-phase channel pressure drop.
 - GDL transport resistance transition from dry to wet and thermal conductivity as a function of saturation.
 - Local oxygen transport resistance decreases with decreasing ionomer film thickness, albeit with increasing proton transport resistance.
 - Local oxygen transport resistance correlated to both Pt surface area and the surface area of ionomer film that covers Pt/C catalyst.
- **Down-the-channel 1+1D model improved with new relationships integrated**
 - Performance and water balance prediction improved based on a comparison to baseline validation data.
 - Model refinement underway for better agreement to the AC validation data.
- **Database updated**
 - Visit www.PEMFCdata.org (development will continue throughout the project). Data are being utilized by at least 3 DOE sponsored projects and 1 EU sponsored DECODE project. Numerous academic leaders and graduate students have contacted us with intent for using the database to supplement their research.

Future Work

- **Finalize wet 1+1D model**
 - Focus on the cathode catalyst layer liquid water model to improve current distribution prediction of the auto-competitive material set.
- **Wrap-up component characterization and modeling**
 - Link findings from various ionomer studies and identify a critical path forward.
 - Document component models and provide a clear linkage to the 1-D resistance used in the finalized model.
- **Reporting**
 - Based on parametric studies using the finalized model, make recommendations for key focus areas to improve next generation PEMFC technology.
 - Publish data for public use through on-line database and peer-reviewed journals.

Acknowledgements



DOE

- David Peterson
- Donna Ho

General Motors

- Aida Rodrigues
- David Caulk (formerly)
- Shawn Clapham (formerly)
- Nalini Subramanian (formerly)
- Rob Reid (formerly)
- Matthew Dioguardi (formerly)
- Rob Moses (formerly)
- Thomas Migliore (formerly)
- Amanda Demitrish
- Bonnie Reid
- Tiffany Williamson (formerly)
- Thomas Greszler (formerly)
- Steve Goebel (formerly)
- David Curran (formerly)
- Matt Albee
- Ted Gacek (formerly)
- Jacqueline Sergi (formerly)

Penn State

- Stephanie Petrina
- Shudipto Dishari
- Cory Trivelpiece
- David Allara
- Tom Larrabee

Roch. Inst. of Tech

- Guangsheng Zhang
- Ting-Yu Lin
- Michael Daino
- Evan See
- Rupak Banerjee
- Jeet Mehta
- Mustafa Koz
- Preethi Gopalan
- Matthew Garafalo

NIST

- Eli Baltic
- Joe Dura

Univ. of TN Knoxville

- Jake LaManna
- Feng-Yuan Zhang
- Subhadeep Chakraborty
- Ahmet Turhan
- Susan Reid
- Colby Jarrett
- Michael Manahan

Univ. of Rochester

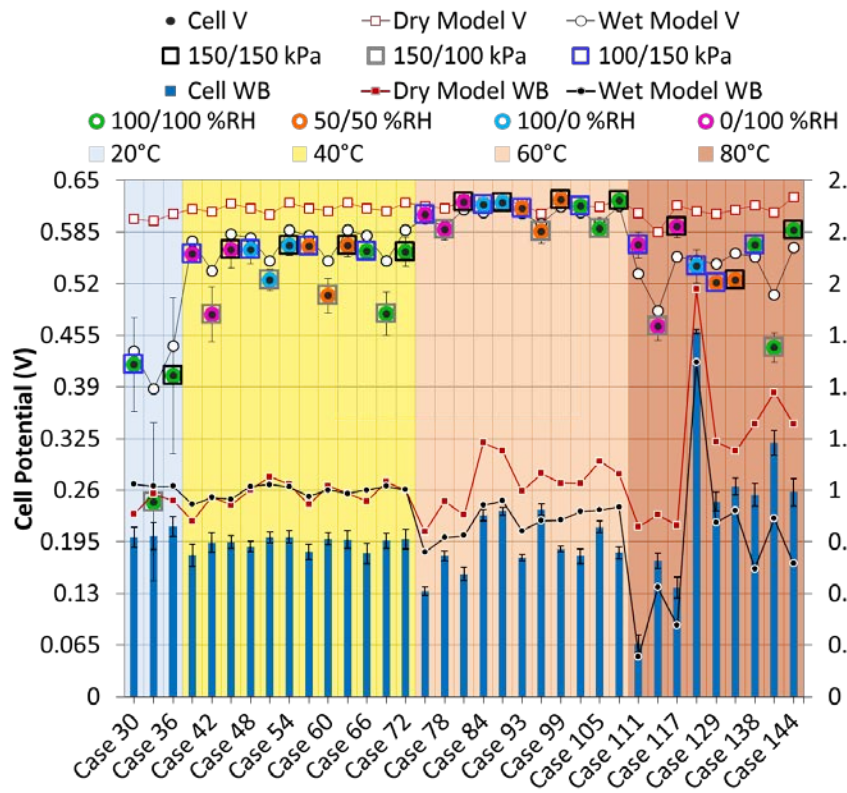
- Yiuxu Liu
- Darcy Chen



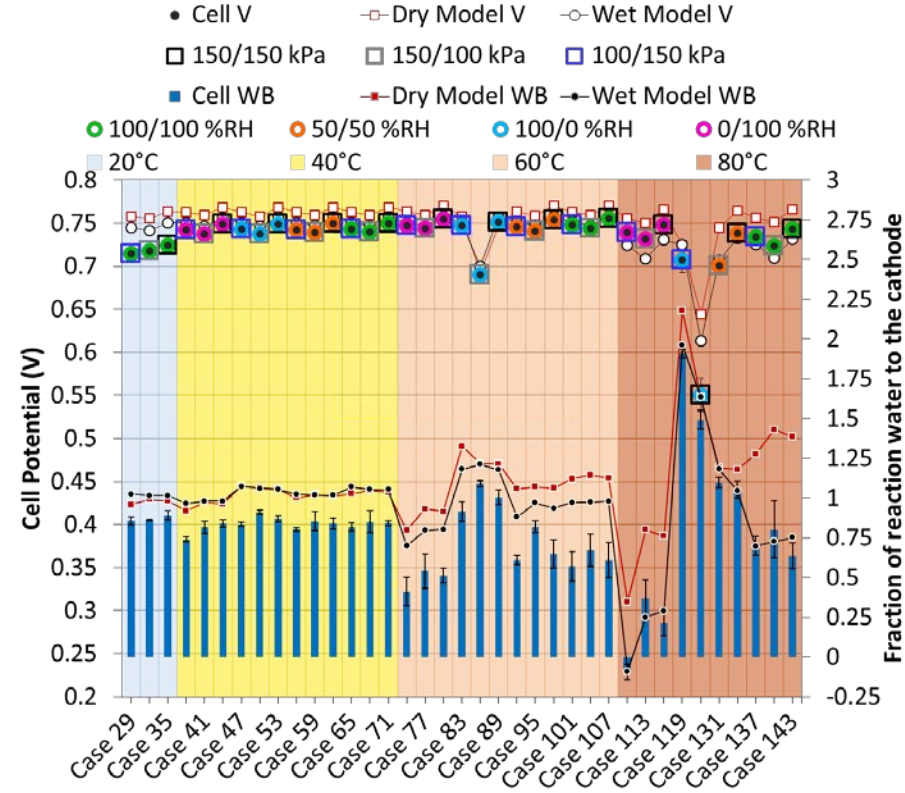
Current Status of Wet 1+1D Model – Baseline Material Set

Error Bars are 95% Confidence Intervals for the Mean

1.5 A/cm² Test Cases



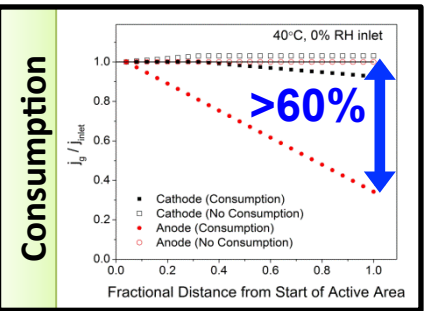
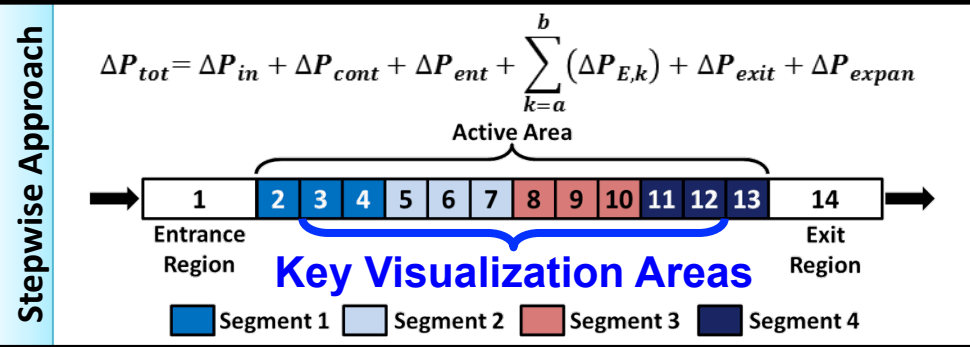
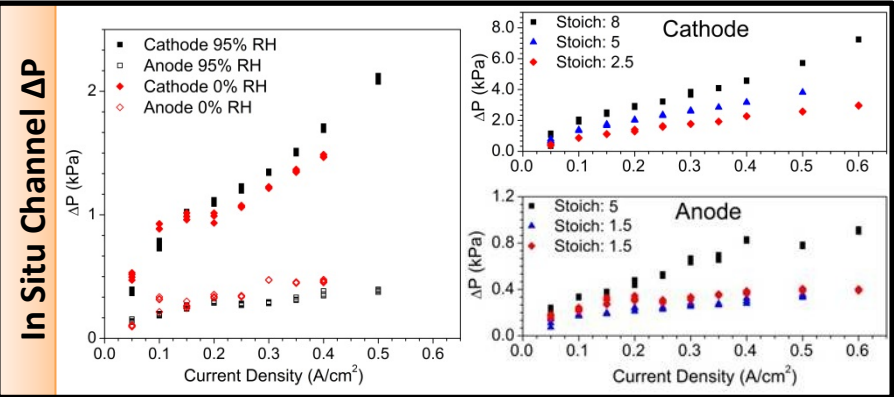
0.4 A/cm² Test Cases



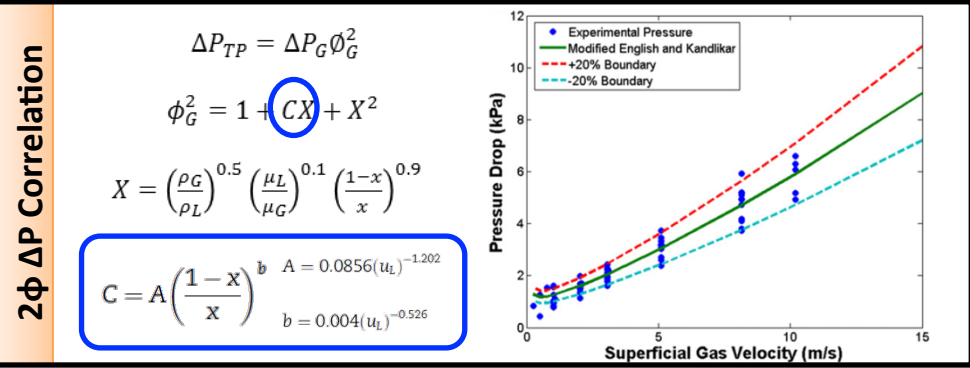
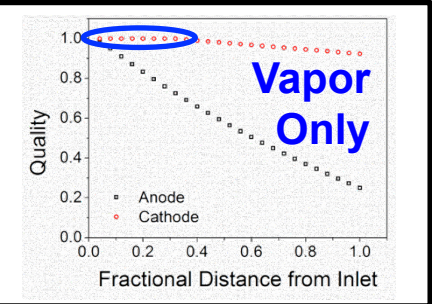
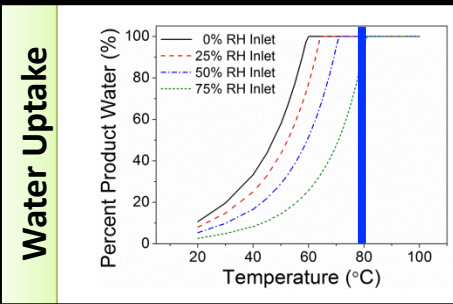
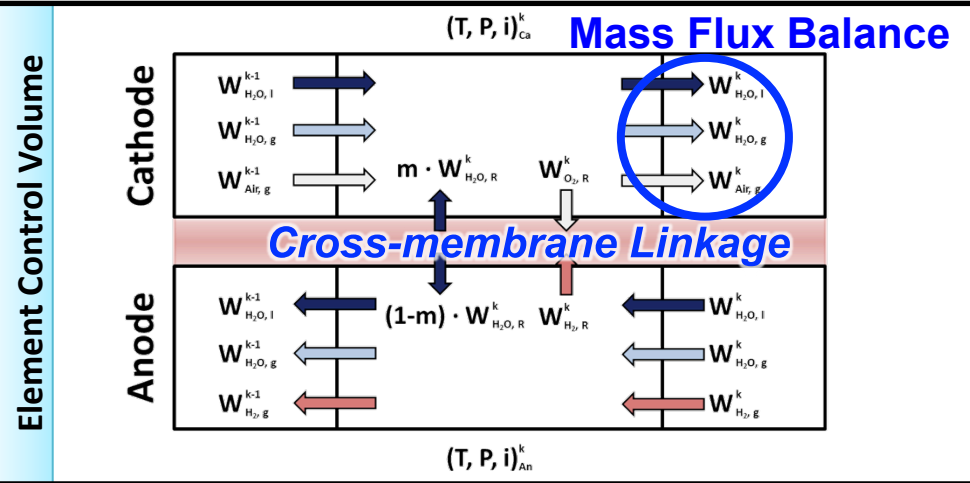
- Predicted cell voltage agrees well with data for 0.1 A/cm² test cases in which no water balance data is available.
- Model is being improved by incorporating newly developed relationships from component studies.

Two-Phase ΔP Modeling Scheme

Unique modeling scheme based on stepwise procedure incorporating local water saturation and cross-membrane transport.



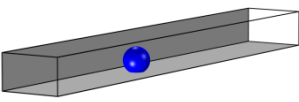
- Cross-membrane Water Transport**
- Major mechanisms
 - Electro-osmotic drag
 - Back diffusion
 - Hydraulic permeation
 - Thermal-osmotic drag
 - Net water to cathode
 - Directly proportional to net drag coefficient



The Effect of Droplets and Films on Interfacial O₂ Resistance

Fully developed $Sh=3.35$ (Baseline Channels)

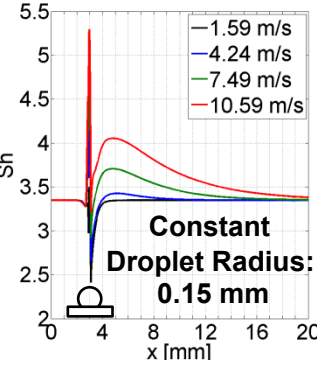
Single Droplet



- Sh increases with air velocity and droplet radius
- Maximum Sh increase in the droplet wake: **21%**

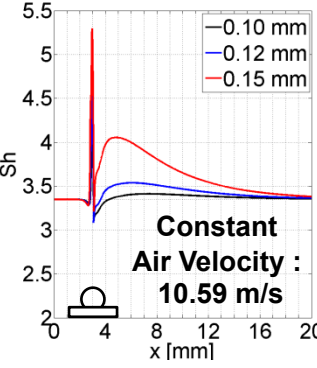
Constant Droplet Radius: **0.15 mm**

Legend: 1.59 m/s, 4.24 m/s, 7.49 m/s, 10.59 m/s

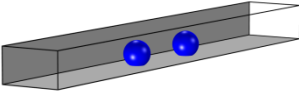


Constant Air Velocity: **10.59 m/s**

Legend: 0.10 mm, 0.12 mm, 0.15 mm



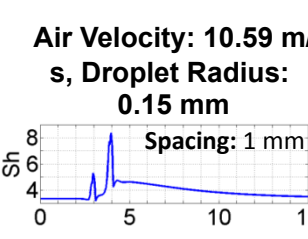
Two Droplets



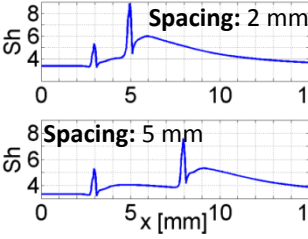
- Maximum Sh increase (**78%**) in the droplet wake with **2 mm** spacing

Air Velocity: **10.59 m/s**, Droplet Radius: **0.15 mm**

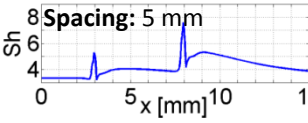
Spacing: **1 mm**



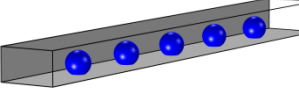
Spacing: **2 mm**



Spacing: **5 mm**

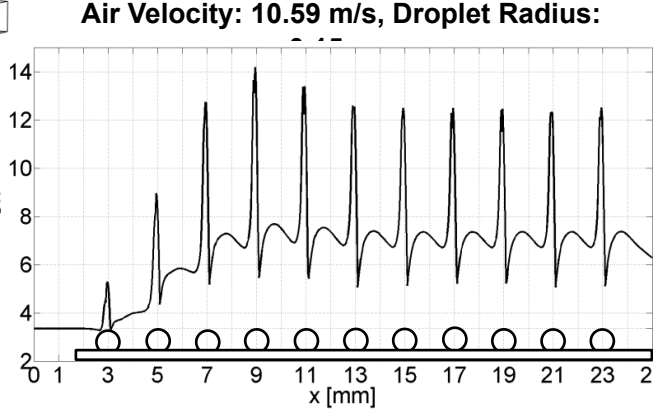


Multiple Droplets



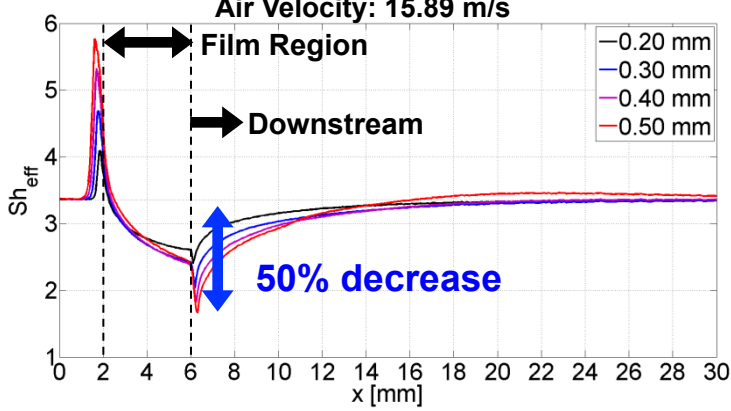
- Significant increase in Sh for the **first 4** droplets
- Average Sh increases to **123%**

Air Velocity: **10.59 m/s**, Droplet Radius: **0.15 mm**



Film Width

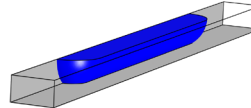
Air Velocity: **15.89 m/s**



Legend: 0.20 mm, 0.30 mm, 0.40 mm, 0.50 mm

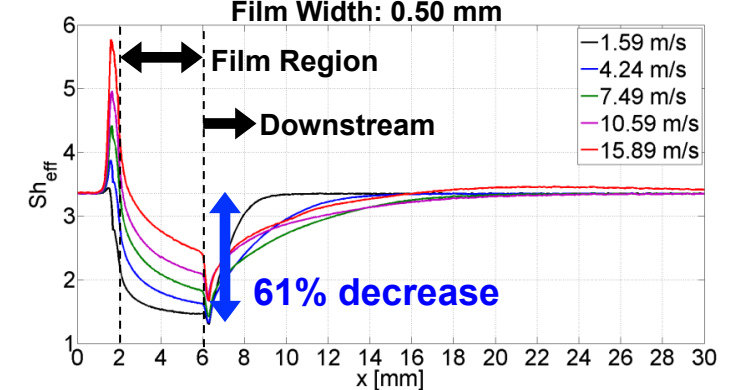
Annotations: Film Region, Downstream, **50% decrease**

- Sh_{eff} in film and wake regions **decreases** with film width.
- Decrease in Sh_{eff} persists in film wake for **~2 film lengths**



Films - Air Velocity

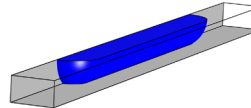
Film Width: **0.50 mm**



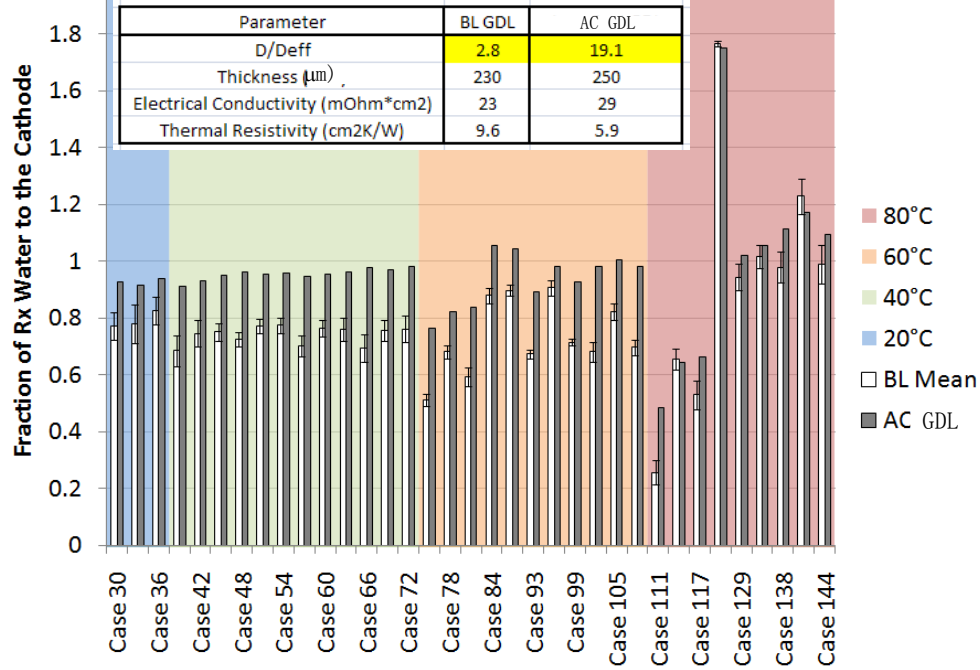
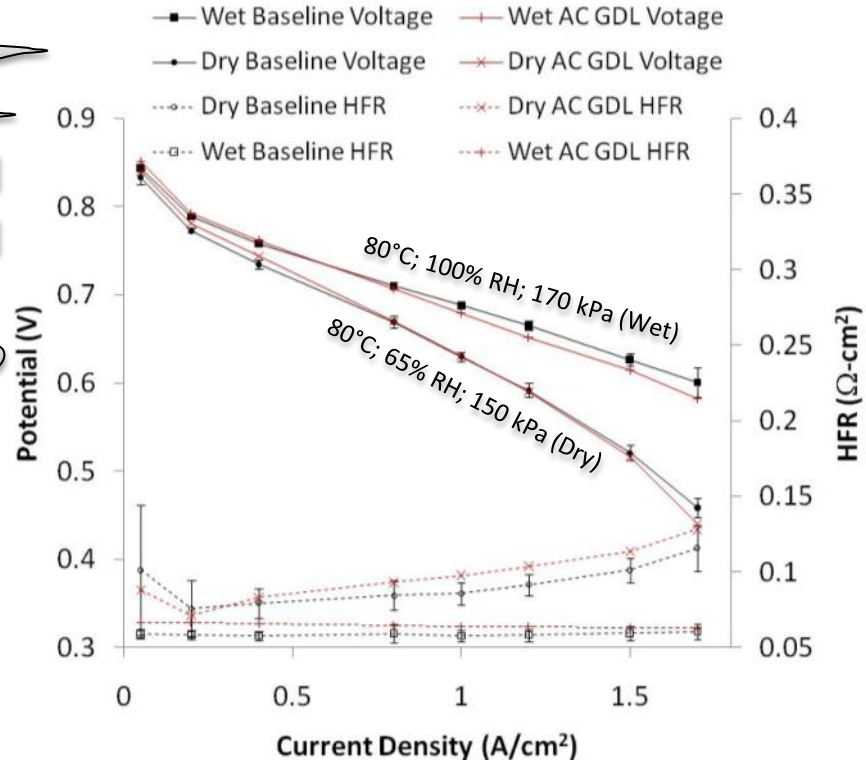
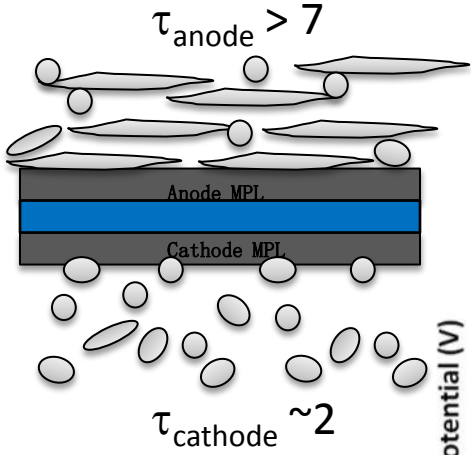
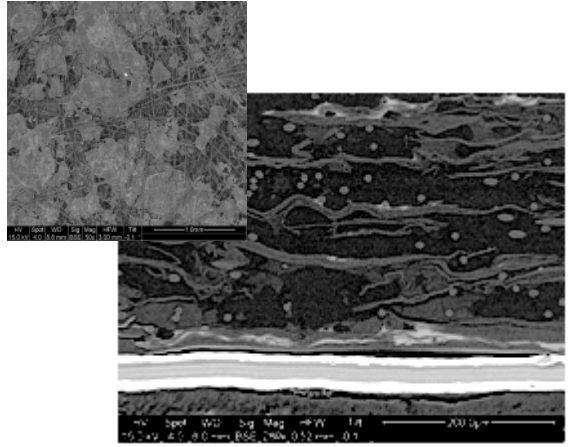
Legend: 1.59 m/s, 4.24 m/s, 7.49 m/s, 10.59 m/s, 15.89 m/s

Annotations: Film Region, Downstream, **61% decrease**

- Air velocity impacts Sh_{eff}
 - **positively** in the **film** region.
 - **negatively** in the **wake** region.
- Decrease in Sh_{eff} persists in film wake for **~1-2 film lengths**



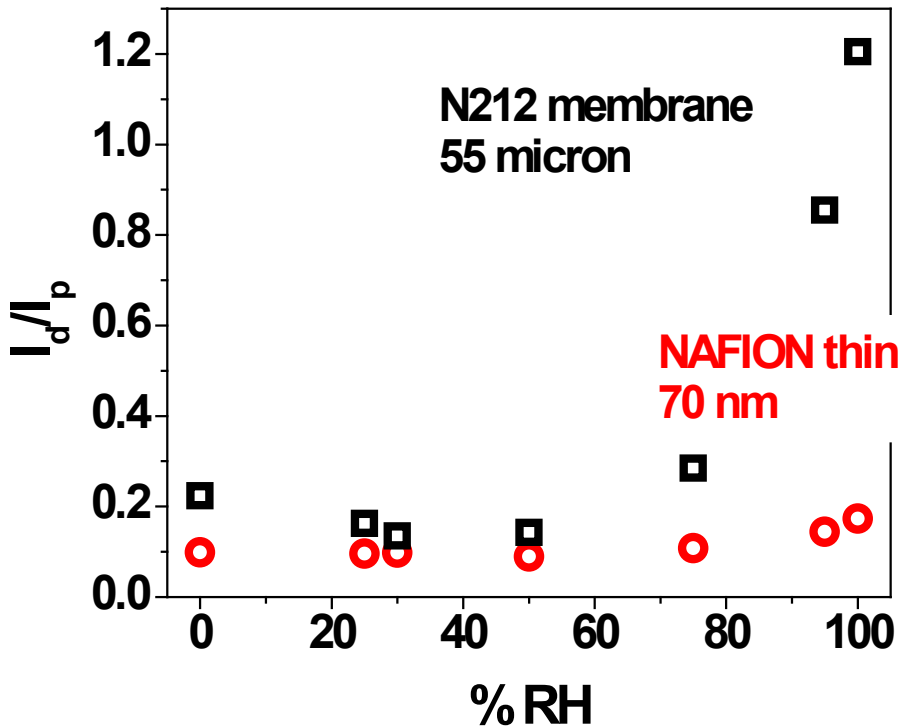
Offsetting Water Balance with High Diffusion Resistance GDL



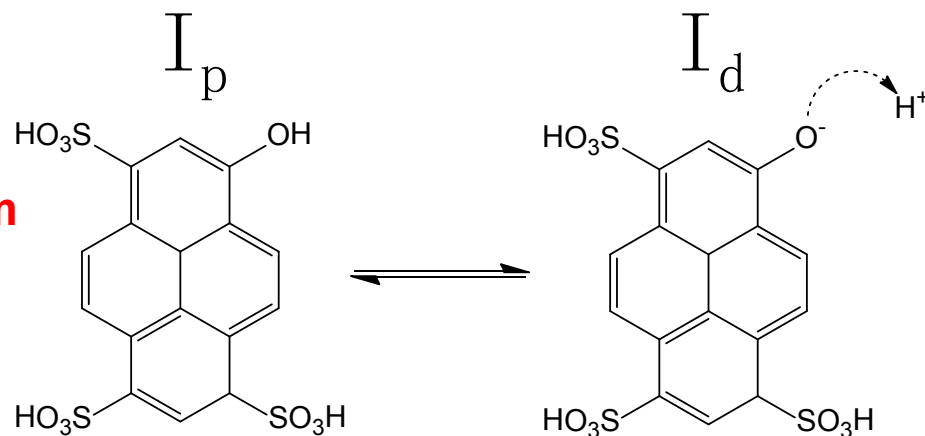
Liquid water in the anode subsystem has a negative impact on efficiency and cold start performance. This material change significantly shifts the water balance toward the cathode without changing performance. Additionally, the "AC GDL" consists of lower cost precursor materials combined with a lower carbonization temperature. This material has an estimated cost reduction of 40% in comparison with typical GDL materials. Patent pending.

Proton Activity in Thin Films

Equivalent λ in these samples



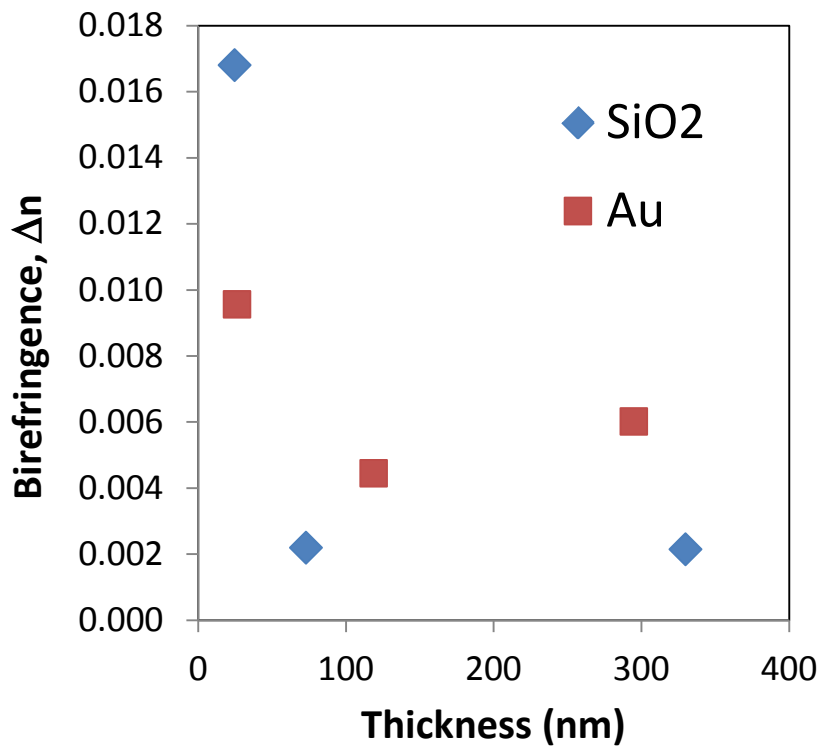
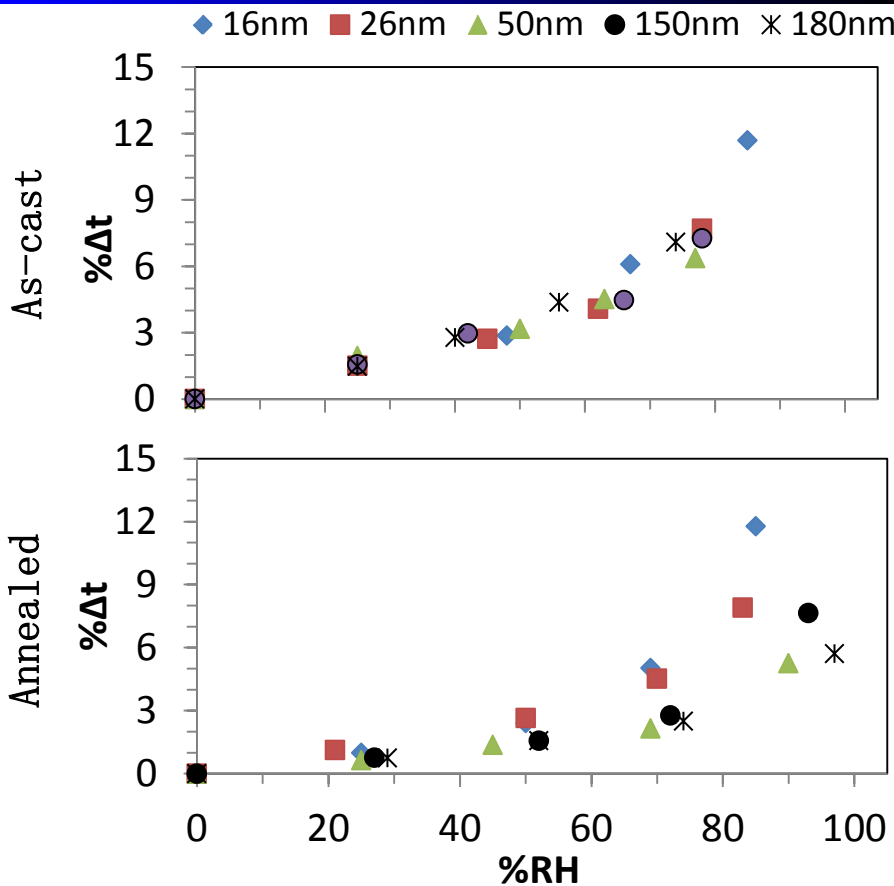
Photoacid Dye Probes Proton Activity by Measuring Dye Dissociation



Lower proton activity (fewer solvated protons from dye) in thinner films as revealed by photoacid fluorescence. Related to thin film structure and could change proton availability for ORR. Disordered domains in thin films may cause ion pairing and change the nature of the catalyst particle/ionomer interface.

Dishari, S. K., M. A. Hickner, "Confinement and Proton Transfer in NAFION[®] Thin Films," *Macromolecules* **2013**, 46(2), 413-421.

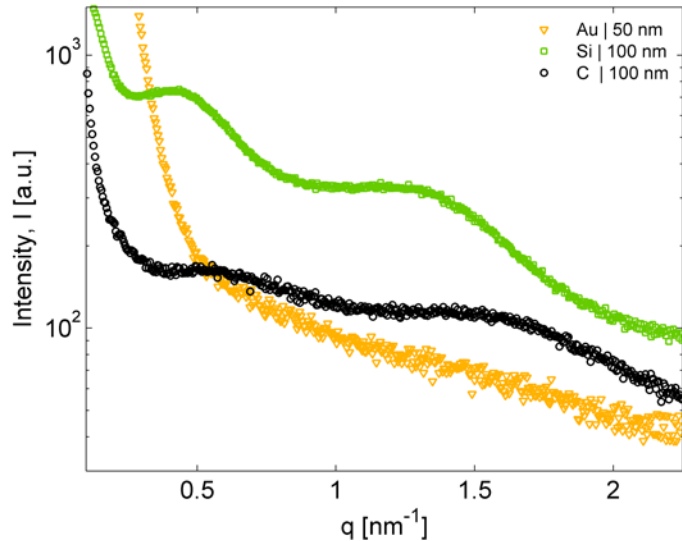
Heat Treatment and Alignment in Thin Films



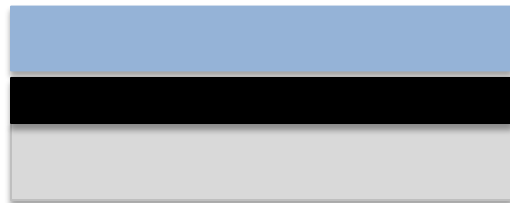
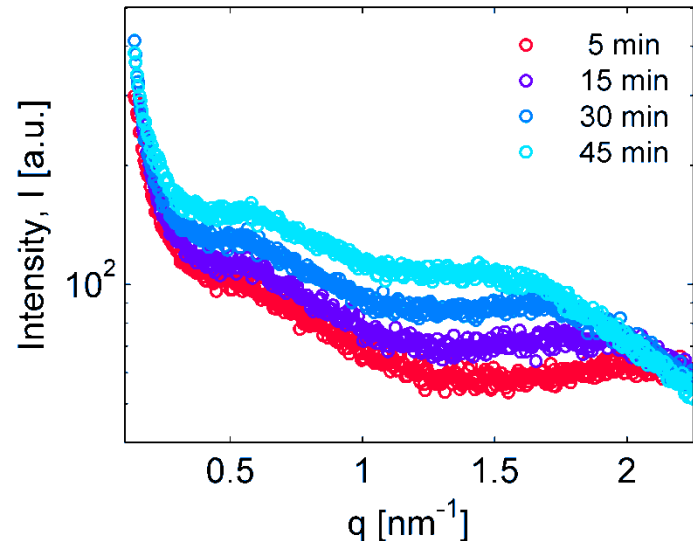
As-cast and heat treated films thinner than about 30 nm show comparable swelling as a function of RH. Thicker films were able to re-arrange. This result indicates strong confinement of thin films that cannot re-arrange upon heating which could have ramifications on electrode performance and structure. Birefringence as a function of thickness showed more strongly aligned films on SiO₂ demonstrate strong SiO₂/Nafion[®] interactions compared to less aligned films on Au which have weak binding to Nafion[®].

Thin Polymer Films on Carbon Surfaces

Different ionic domain features on Au, C, and Si



Swelling of 100 nm Nafion® thin film on carbon



Nafion®
Pyrolyzed carbon
Si substrate

- Polyfurfuryl alcohol (PFA) is spun-cast onto a Si wafer and pyrolyzed
- Resulting surfaces characterized by Raman and ellipsometry

| Carbon precursor concentration | Average thickness (nm) |
|--------------------------------|------------------------|
| 1 % PFA | 2.4 +/- 0.05 |
| 5 % PFA | 8.1 +/- 0.07 |
| 9 % PFA | 17.9 +/- 1.14 |

- Sample fabrication at Penn State
- Scattering at LBL with Ahmet Kusoglu and Adam Weber